Design, synthesis, biological evaluation and molecular docking study of novel thieno[3,2-*d*]pyrimidine derivatives as potent FAK inhibitors

Ruifeng Wang, Sijia Yu, Xiangxin Zhao, Yixuan Chen, Bowen Yang, Tianxiao Wu, Chenzhou Hao, Dongmei Zhao, Maosheng Cheng

PII: S0223-5234(19)31182-1

DOI: https://doi.org/10.1016/j.ejmech.2019.112024

Reference: EJMECH 112024

To appear in: *European Journal of Medicinal Chemistry*

Received Date: 20 October 2019

Revised Date: 13 December 2019

Accepted Date: 29 December 2019

Please cite this article as: R. Wang, S. Yu, X. Zhao, Y. Chen, B. Yang, T. Wu, C. Hao, D. Zhao, M. Cheng, Design, synthesis, biological evaluation and molecular docking study of novel thieno[3,2-*d*]pyrimidine derivatives as potent FAK inhibitors, *European Journal of Medicinal Chemistry* (2020), doi: https://doi.org/10.1016/j.ejmech.2019.112024.

Graphical abstract

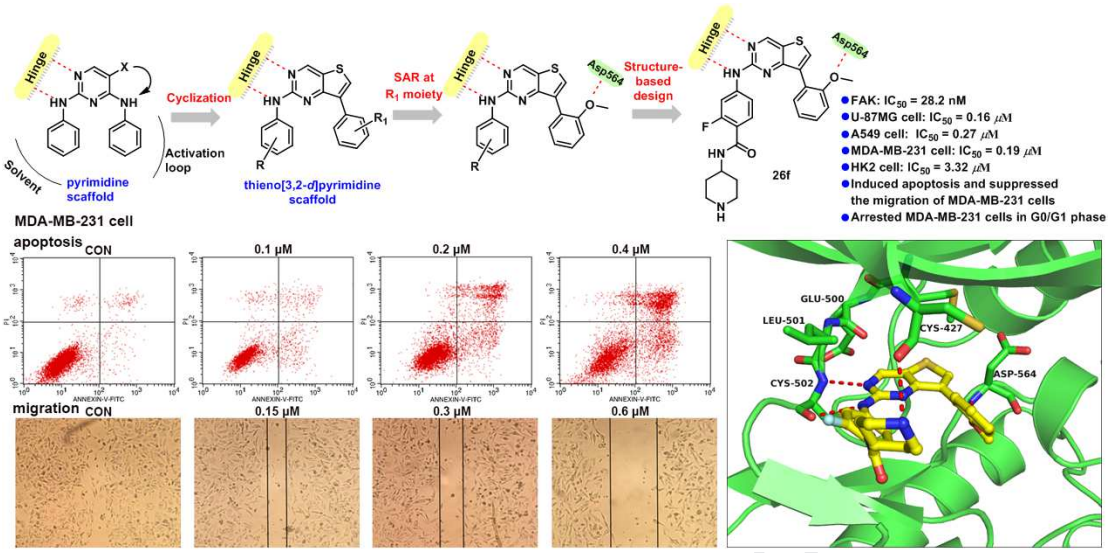

Design, synthesis, biological evaluation and molecular docking study of novel thieno[3,2-*d*]pyrimidine derivatives as potent FAK inhibitors

Ruifeng Wang[a], Sijia Yu[a], Xiangxin Zhao[a], Yixuan Chen[a, b], Bowen Yang[a], Tianxiao Wu[a], Chenzhou Hao[a], Dongmei Zhao[a,*], Maosheng Cheng[a]

[a] Key Laboratory of Structure-Based Drug Design and Discovery, Ministry of Education, School of Pharmaceutical Engineering, Shenyang Pharmaceutical University, 103 Wenhua Road, Shenhe District, Shenyang, 110016, China

[b] The School of life Science and Biopharmaceutical, Shenyang Pharmaceutical University, 103 Wenhua Road, Shenhe District, Shenyang, 110016, China

[*]Corresponding author

E-mail address: medchemzhao@163.com (D. Zhao).

Abstract

A series of 2,7-disubstituted-thieno[3,2-*d*]pyrimidine derivatives were designed, synthesized and evaluated as novel focal adhesion kinase (FAK) inhibitors. The novel 2,7-disubstituted-thieno[3,2-*d*]pyrimidine scaffold has been designed as a new kinase inhibitor platform that mimics the bioactive conformation of the well-known diaminopyrimidine motif. Most of the compounds potently suppressed the enzymatic activities of FAK and potently inhibited the proliferation of U-87MG, A-549 and MDA-MB-231 cancer cell lines. Among these derivatives, the optimized compound **26f** potently inhibited the enzyme (IC_{50} = 28.2 nM) and displayed stronger potency than TAE-226 in U-87MG, A-549 and MDA-MB-231 cells, with IC_{50} values of 0.16, 0.27, and 0.19 μM, respectively. Compound **26f** also exhibited relatively less cytotoxicity (IC_{50} = 3.32 μM) toward a normal human cell line, HK2. According to the flow cytometry results, compound **26f** induced the apoptosis of MDA-MB-231 cells in a dose-dependent manner and effectively arrested MDA-MB-231 cells in G0/G1 phase. Further investigations revealed that compound **26f** potently suppressed the migration of MDA-MB-231 cells. Collectively, these data support the further development of compound **26f** as a lead compound for FAK-targeted anticancer drug discovery.

Keywords: FAK inhibitor, Thieno[3,2-*d*]pyrimidine, Structure-activity relationship, Apoptosis, Migration.

1. Introduction

Focal adhesion kinase (FAK) is an intracellular non-receptor tyrosine kinase that is activated by integrins or growth factor receptors in various types of human cancers[1]. Accumulating evidence indicates that FAK plays significant roles in survival, motility, metastasis, adhesion, lymphangiogenesis, angiogenesis, the tumour microenvironment, cancer stem cell functions and the epithelial-to-mesenchymal transition[2-6]. Overexpression of FAK has been clinically observed in primary human hepatocellular carcinomas[7], human colorectal carcinomas[8], human ovarian carcinomas[9] and human breast cancers[10], implicating a role of FAK in cancer development. The overexpression and activation of FAK have been investigated primarily in primary or metastatic cancers and correlate with poor clinical outcomes[11-12]. Furthermore, recent research has identified FAK as a key mediator of the immune response in certain cancers and provides strong evidence that FAK inhibitors may trigger immune-mediated tumour regression, revealing previously unrecognized therapeutic opportunities[13-14]. The mechanisms of FAK activation and signalling have been extensively studied, with FAK being highlighted as a potential target for anticancer therapeutics.

Given the upregulation of FAK in cancer, several agents are logically being developed to target FAK for cancer therapy. In particular, many small molecule inhibitors have been designed and developed to directly block

ATP-kinase interactions. As shown in **Figure 1**, TAE226[15] exhibits antitumour activity *in vitro* and *in vivo* against several types of malignant tumours and is often used as a positive reference compound in research. In addition, several FAK inhibitors are being evaluated in clinical trials at different stages, including VS-4718 (**2**, phase I)[16], CEP-37440 (**3**, phase I)[17], GSK2256098 (**4**, phase II)[18], PF-562271 (**5**, phase I)[19], and defactinib (**6**, phase II)[20], among others. These compounds have exhibited potent inhibition of FAK and potent antitumour activities in a panel of *in vitro* and *in vivo* cancer models.

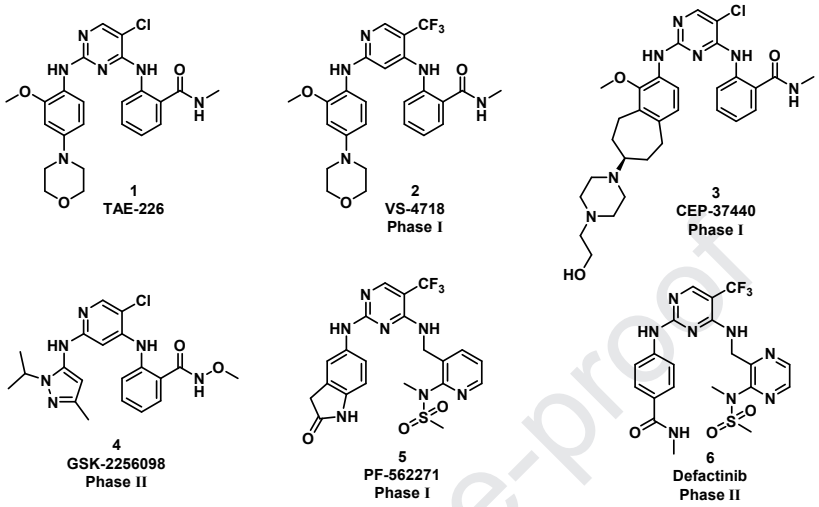

Figure 1. Structures of potent and selective FAK inhibitors.

Among the scaffolds of currently available FAK inhibitors, the 2,4-diaminopyridine and 2,4-diaminopyrimidine scaffolds are the major scaffolds used in compounds described by pharmaceutical companies and academic research institutions[21-22]. A general representation of the diaminopyrimidine motif at the ATP active site of the kinase is shown in **Figure 2**. The diaminopyrimidine derivatives bind to the ATP-binding site of FAK by adopting a U-shaped ligand conformation. The compounds are anchored to the hinge region by double-dentate hydrogen bonding of the pyrimidine nitrogen and aniline NH to the hinge region. Moreover, the aryl residues back toward the DFG motif of activation loop and orient toward solvent region. We postulated that we could take advantage of the active site conformation of this pharmacophore to further diversify the chemical space by constraining the core structure and orienting the side chains into bioactive trajectories. Based on a cyclization strategy, a novel 2,7-disubstituted-thieno[3,2-*d*]pyrimidine scaffold was designed as a novel kinase inhibitor platform that mimics the bioactive conformation of the well-known diaminopyrimidine motif. To the best of our knowledge, no thieno[3,2-*d*]pyrimidine derivatives serving as FAK inhibitors have been reported, and a systematic investigation of the effects of substitutions has not yet been conducted. In addition, the SAR of these compounds was discussed in this manuscript, and various substituents with hydrogen bond receptors were introduced at R_1 to form hydrogen bond interactions with Asp564 of the DFG motif. Based on the SAR at R_1, we decided to introduce an *o*-methoxyl group at the R_1 position and explore the R_2, R_3, R_4 and R_5 positions to obtain a series of potent FAK inhibitors using a structure-based drug design approach.

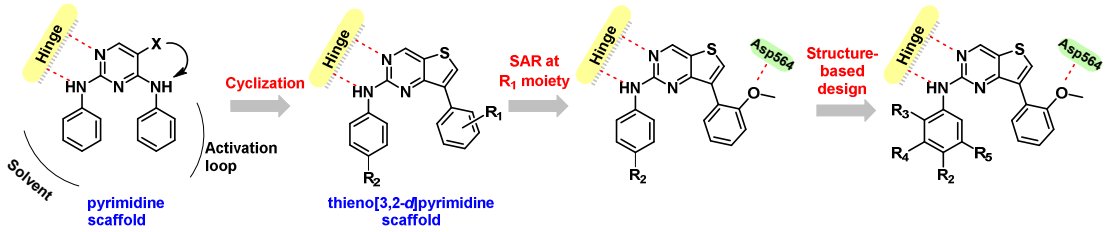

Figure 2. Design of the target compounds.

2. Chemistry

Compounds **11a-h** and intermediates **14**, **17**, **20** and **23** were synthesized using the method depicted in **Scheme 1**. Palladium-catalysed regioselective dechlorination of 2,4-dichlorothieno[3,2-*d*]pyrimidine (**7**) in the presence of Na_2CO_3 occurred exclusively at the C-4 position[23], and electrophilic iodization of compound **8** using NIS in AcOH yielded the desired C-7 iodine intermediate **9**. Intermediates **10a-h** were obtained in a rapid and efficient manner *via* Suzuki coupling of compound **9** with the corresponding boric acid or borate. Palladium-catalysed Buchwald cross-coupling with dimethyl(4-aminobenzyl)phosphonate afforded compounds **11a-h**[24]**.** Acetylation of 3-bromoaniline (**12**) followed by Suzuki coupling with bis(pinacolato)diboron generated intermediate **14**[25]. Compound **12** was reacted with methanesulfonyl chloride to yield intermediate **15.** Subsequent methylation yielded the N-methyl sulfonamide **16**. Treatment with bis(pinacolato)diboron and $Pd(dppf)Cl_2$ produced the required Suzuki coupling partner[26], intermediate **17**. 3-Bromobenzoic acid (**18**) was converted into an acid chloride and condensed with methylamine to produce intermediate **19**, a subsequent Suzuki coupling reaction with bis(pinacolato)diboron afforded intermediate **20**. Commercially available 1-(chloromethyl)-4-nitrobenzene (**21**) was reacted with trimethyl phosphate to provide the dimethyl (4-nitrobenzyl)phosphonate (**22**), which was reduced under P/C-H_2 conditions to form the aniline **23**.

Compounds **24a-j**, **26a-i**, **27a-b**, and **28c-g** were prepared using similar reaction conditions as depicted in **Scheme 2.** The synthesis of compounds **26a-i** was used as an example for illustration. Buchwald cross-coupling of compound **10a** with appropriate substituted amines in the presence of $Pd(dba)_2$, BINAP and Cs_2CO_3 or $Pd(AcO)_2$, X-phos and Cs_2CO_3 yielded the intermediates **25a-i**. Then, the Boc group was subsequently removed under acidic conditions to produce compounds **26a-i**.

Intermediates **31a-f**, **34a-g**, **36**, **38** and **40** were synthesized as depicted in **Scheme 3**. Intermediates **31a-f** and **34a-g** were synthesized using a two-step synthetic approach according to our previously reported methods[27]. 1-(chloromethyl)-4-nitrobenzene (**21**) was reacted with triethyl phosphate to provide the diethyl (4-nitrobenzyl)phosphonate (**35**)[28], followed by a reduction of nitro (H_2, Pd/C) to generate intermediate **36**. Additionally, compound **35** was treated with oxalyl chloride and then directly reacted with morpholine or CH_3NH_2•HCl in the presence of TEA base to prepare the phosphoramide intermediates **37** and **39**, which were reduced under P/C-H_2 conditions to form the anilines **38** and **40**.

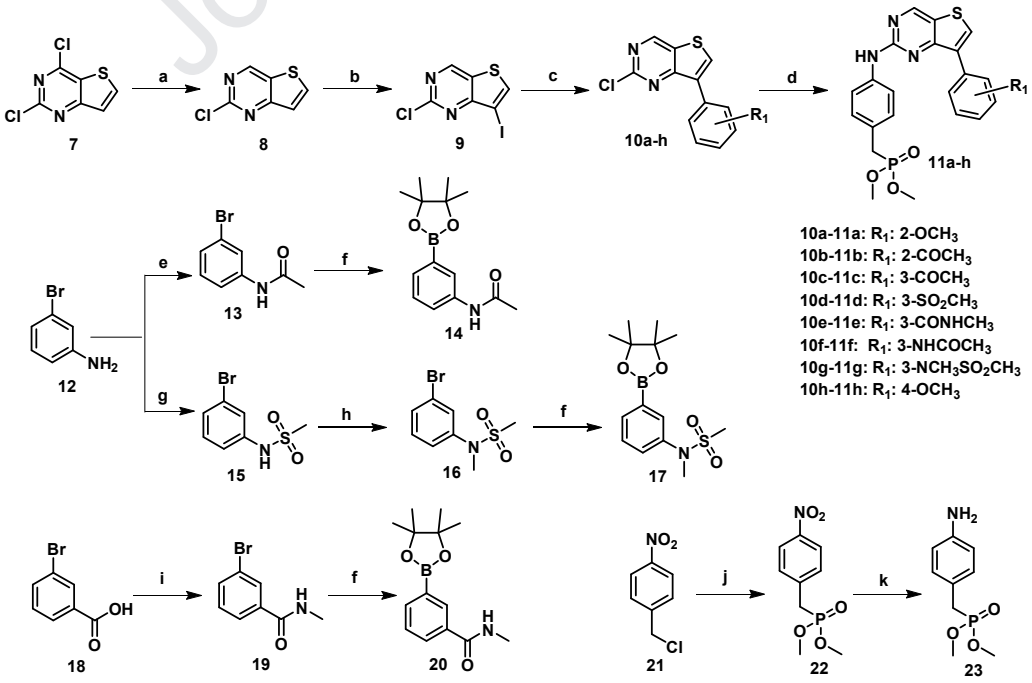

Scheme 1. Synthesis of compounds **11a-h** and intermediates **14**, **17**, **20** and **23**. Reagents and conditions: (a) Pd/C, H_2, Na_2CO_3, EtOH, 30 °C; (b) NIS, CH_3COOH, 80 °C; (c) corresponding boric acid or borate, $Pd(dppf)Cl_2$, K_2CO_3, 1,4-dioxane/H_2O, 90 °C; (d) dimethyl (4-aminobenzyl)phosphonate, $Pd(AcO)_2$, X-phos, Cs_2CO_3, dioxane, 90 °C; (e) acetic anhydride, TEA, CH_2Cl_2, rt; (f) Bis(pinacolato)diboron, $Pd(dppf)Cl_2$, AcOK, dioxane, 80 °C; (g) methanesulfonyl chloride, pyridine, CH_2Cl_2, 0 °C; (h) CH_3I, K_2CO_3, DMF, rt; (i) I) oxalyl chloride, DMF, CH_2Cl_2, 60 °C; II) CH_3NH_2•HCl, TEA, CH_2Cl_2, rt; (j) trimethyl phosphite, 120 °C; and (k) Pd/C, H_2, EtOH, 40 °C.

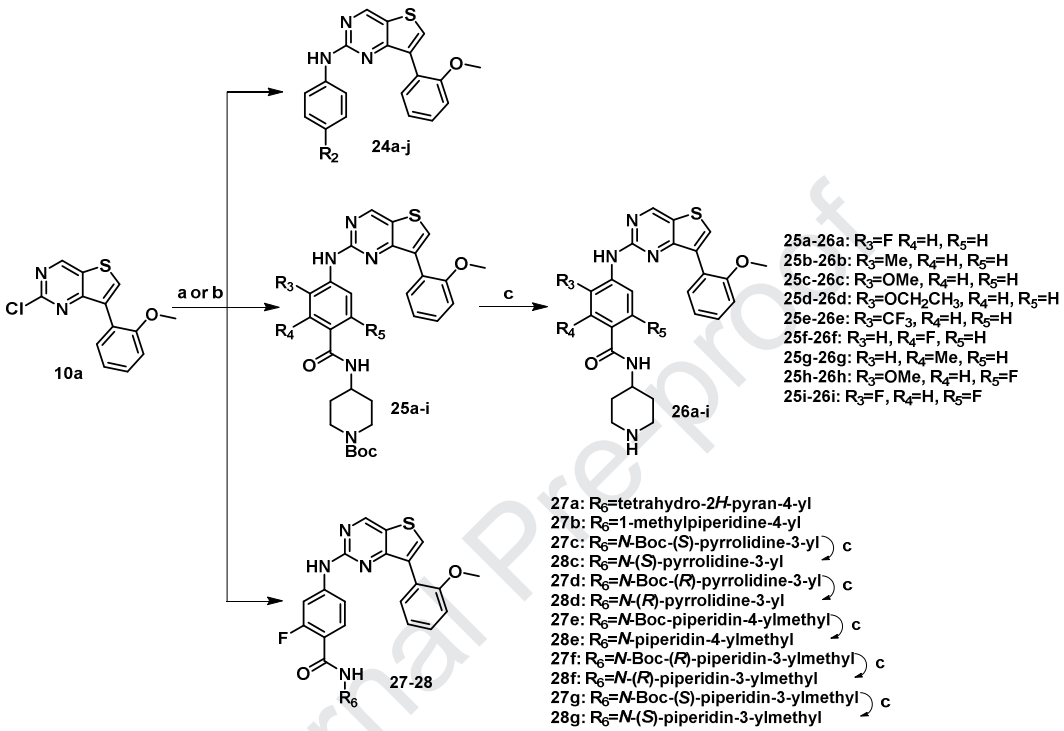

Scheme 2. Synthesis of compounds **24a-j**, **26a-i**, **27a-b** and **28c-g**. Reagents and conditions: (a) corresponding aromatic amines, $Pd(AcO)_2$, X-phos, Cs_2CO_3, dioxane, 90 °C; (b) corresponding aromatic amines, $Pd(dba)_2$, BINAP, Cs_2CO_3, dioxane, 90 °C; and (c) HCl-EA, rt.

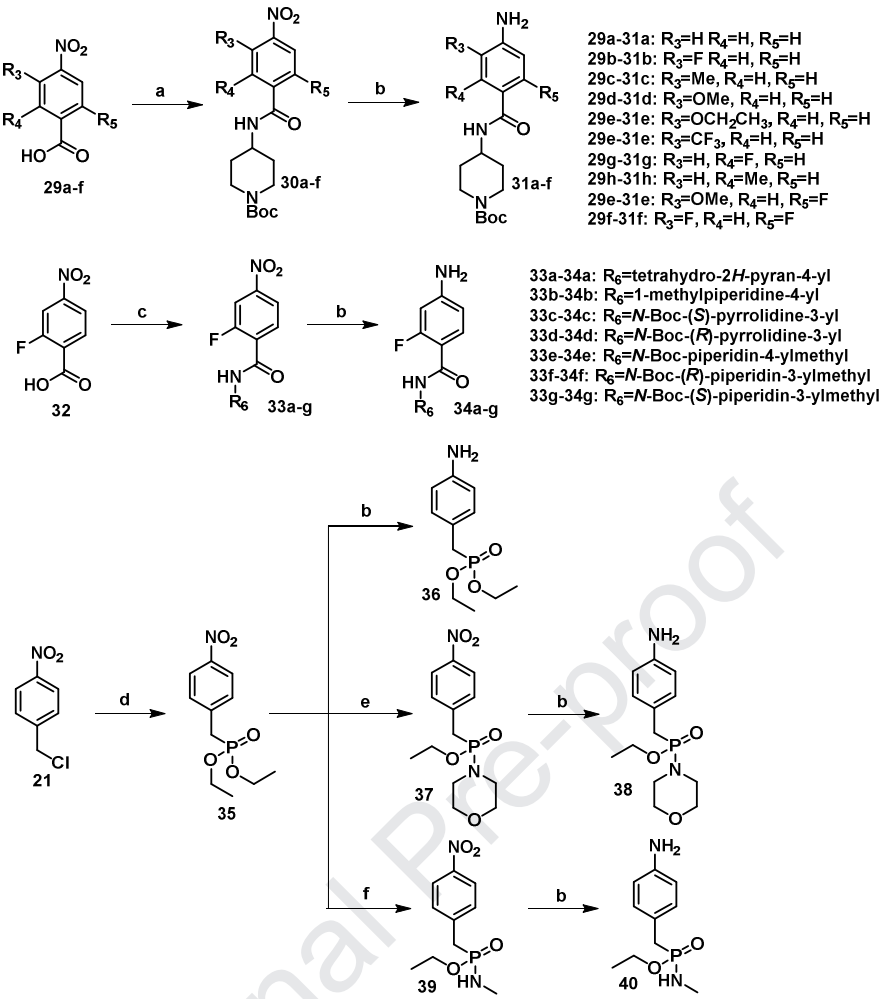

Scheme 3. Synthesis of intermediates **31a-f**, **34a-g**, **36**, **38** and **40**. Reagents and conditions: (a) tert-butyl 4-aminopiperidine-1-carboxylate, HATU, DIPEA, CH_2Cl_2, 25–40 °C; (b) Pd/C, H_2, EtOH, 40 °C; (c) R_6-NH_2, HATU, DIPEA, CH_2Cl_2, 25–40 °C; (d) triethyl phosphite, 130 °C; (e) I) oxalyl chloride, DMF, CH_2Cl_2, 60 °C; II) morpholine, TEA, CH_2Cl_2, rt; and (f) I) oxalyl chloride, DMF, CH_2Cl_2, 60 °C; II) CH_3NH_2•HCl, TEA, CH_2Cl_2, rt.

3. Results and discussion

3.1. Biological evaluation and analysis of the structure-activity relationship

All newly synthesized compounds were evaluated for their activities against the FAK enzyme using homogeneous time-resolved fluorescence (HTRF) assay. Their abilities to inhibit the proliferation of U-87MG (human glioma cancer cell), A549 (human lung cancer cell) and MDA-MB-231 (human breast cancer cell) cell lines, which overexpress FAK [10, 29, 30], were evaluated using the MTT assay. TAE-226 was tested for comparison.

We first focused on the R_1 moiety by fixing the R_2 moiety as a phosphonate group. Different fragments containing hydrogen bond acceptors were introduced at R_1 to form hydrogen bond interactions with Asp564 of the DFG motif. As shown in **Table 1**, most compounds exhibited moderate inhibitory activity against FAK at submicromolar concentrations. In particular, the inclusion of a 2-methoxyl group at R_1 (**11a**) exhibited the strongest inhibition of FAK (IC_{50} = 134.0 nM), whereas switching R_1 to a 2-acetaldehyde group (**11b**) resulted in a marked loss of activity (IC_{50} = 1083 nM). We deduced that the interaction of the C=O bond and C6 of the thieno[3,2-*d*]pyrimidine resulted in an unfavourable conformation of the ligand and that this steric clash resulted in reduced activity. The 3-substituted derivatives (**11c-g**) retained moderate potency against FAK, with IC_{50} values

ranging from 140.1 to 638.4 nM. However, switching the methoxyl group to the para position (**11h**) resulted in a pronounced loss of activity (IC_{50} = 1064 nM).

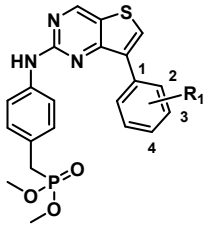

Table 1 The enzymatic activity of FAK in the presence of compounds **11a-h**.

Compd.	R_1	IC_{50} (nM)[a]	Compd.	R_1	IC_{50} (nM)[a]
11a	2-OCH_3	134.0	**11e**	3-$CONHCH_3$	324.5
11b	2-$COCH_3$	1083	**11f**	3-$NHCOCH_3$	377.0
11c	3-$COCH_3$	351.0	**11g**	3-$NCH_3SO_2CH_3$	638.4
11d	3-SO_2CH_3	140.1	**11h**	4-OCH_3	1064
TAE-226		6.3			

[a] The IC_{50} values are presented as the mean (nM) values from two separate experiments.

Compound **11a**, which contained a 2-methoxy group at R_1, exhibited stronger inhibitory activity against FAK than compounds **11b-h**. Thus, we next conducted SAR exploration at the R_2 position, as shown in **Table 2**. The diethyl phosphonate-substituted analogue **24a** (IC_{50} = 156.8 nM) was equally potent as compound **11a**. The incorporation of solubilizing groups into compound **24a** to produce compounds **24b-d** decreased the potency of FAK inhibition, presumably due to the suboptimal location of the methylamino group, hydroxyl group and morpholine ring. The introduction of the *N*-methylformamide group (**24e**), which is identical to defactinib, produced a 2-fold higher potency than exhibited by compound **11a**. Because the para-substitution vector R_2 points toward the solvent region, the introduction of hydrophilic fragments at the R_2 position may increase the activity. A class of hydrophilic fragment-containing derivatives (**24f-j**) bearing an amide linker directly attached to the C_2 phenyl moiety were designed and synthesized. Among these derivatives, the piperidine-4-yl substituted analogues **24f** and **24g** exhibited much higher potency (IC_{50} values of 38.8 and 57.7 nM, respectively) than compound **24e**. However, compounds **24h-j** exhibited lower potency against FAK, with IC_{50} values of 143.6–199.1 nM.

In cell-based assays, most of the target compounds possessed moderate to excellent anticancer activities, with IC_{50} values less than 5.0 μM. Three of these compounds (**24f**, **24h**, and **24i**) potently inhibited the proliferation of U-87MG, A-549 and MDA-MB-231 cancer cell lines, with IC_{50} values ranging from 0.11 to 0.65 μM. Notably, compound **24f**, which had an IC_{50} value of 0.36 μM against A549 cells and of 0.11 μM against MDA-MB-231 cells, was the strongest inhibitor of these two cancer cell lines. Since compound **24f** displayed potent enzymatic and cellular activity, it was selected for molecular docking studies with the FAK crystal structure (PDB: 2JKK). As shown in **Figure 3A**, compound **24f** was located deep in the ATP-binding site, and four H-bonds were observed in the binding mode: two were established between the thieno[3,2-*d*]pyrimidine scaffold and Cys502 in the hinge region of the kinase, another formed between the methoxyl group and Asp564 of the DFG motif, and the fourth formed between NH (piperidine) and Cys427. In addition, as shown in **Figure 3B**, the structural model of the drug-protein complex showed that the binding model of compound **24f** to FAK was similar to that of TAE-226, indicating that the 2,7-disubstituted-thieno[3,2-*d*]pyrimidine scaffold mimicked the bioactive conformation of the well-known diaminopyrimidine motif. Compound **24f** also exhibited good spatial matching with the FAK active pocket (**Figure 3C**). Notably, the gatekeeper+2 residue is a smaller Leu501 in FAK (**Figure 3D**). Therefore, the substituents on the 2-*N*-aryl moiety will occupy the lower hinge area pocket and form a hydrophobic interaction with the side chain of Leu501, thus potentially improving the inhibition of enzyme activity.

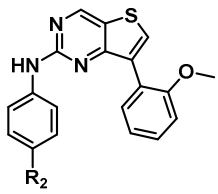

Table 2 Biological activities of compounds **24a-j**.

Compd.	R_2	FAK, IC_{50} (nM)[a]	Antiproliferative activity, IC_{50} (μM)[b]		
			U-87MG	A549	MDA-MB-231
11a		134.0	1.71 ± 0.22	1.80 ± 0.24	7.81 ± 0.22
24a	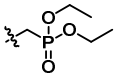	156.8	1.30 ± 0.11	0.96 ± 0.13	4.94 ± 0.14
24b		183.6	1.30 ± 0.07	1.73 ± 0.04	1.21 ± 0.19
24c	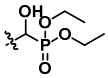	321.5	1.95 ± 0.22	0.35 ± 0.03	2.64 ± 0.23
24d		351.5	1.22 ± 0.14	0.85 ± 0.15	8.35 ± 0.18
24e		79.3	0.71 ± 0.03	0.31 ± 0.02	2.12 ± 0.14
24f	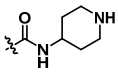	38.8	0.65 ± 0.07	0.36 ± 0.06	0.11 ± 0.01
24g	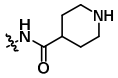	57.7	1.06 ± 0.04	0.45 ± 0.08	1.05 ± 0.11
24h	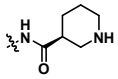	167.1	0.30 ± 0.04	0.50 ± 0.03	0.44 ± 0.03
24i	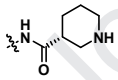	199.1	0.36 ± 0.01	0.41 ± 0.05	0.41 ± 0.05
24j	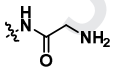	143.6	0.21 ± 0.02	1.95 ± 0.26	2.77 ± 0.19
TAE-226		6.3	1.67±0.02	1.16±0.20	4.06±0.21

[a] The IC_{50} values are presented as the mean (nM) values from two separate experiments.

[b] Concentration that inhibits the proliferation of cancer cells by 50 %. Cell proliferation was measured using the MTT assay after incubation with the compounds for 72 h. The mean values of three independent experiments ± SE are reported.

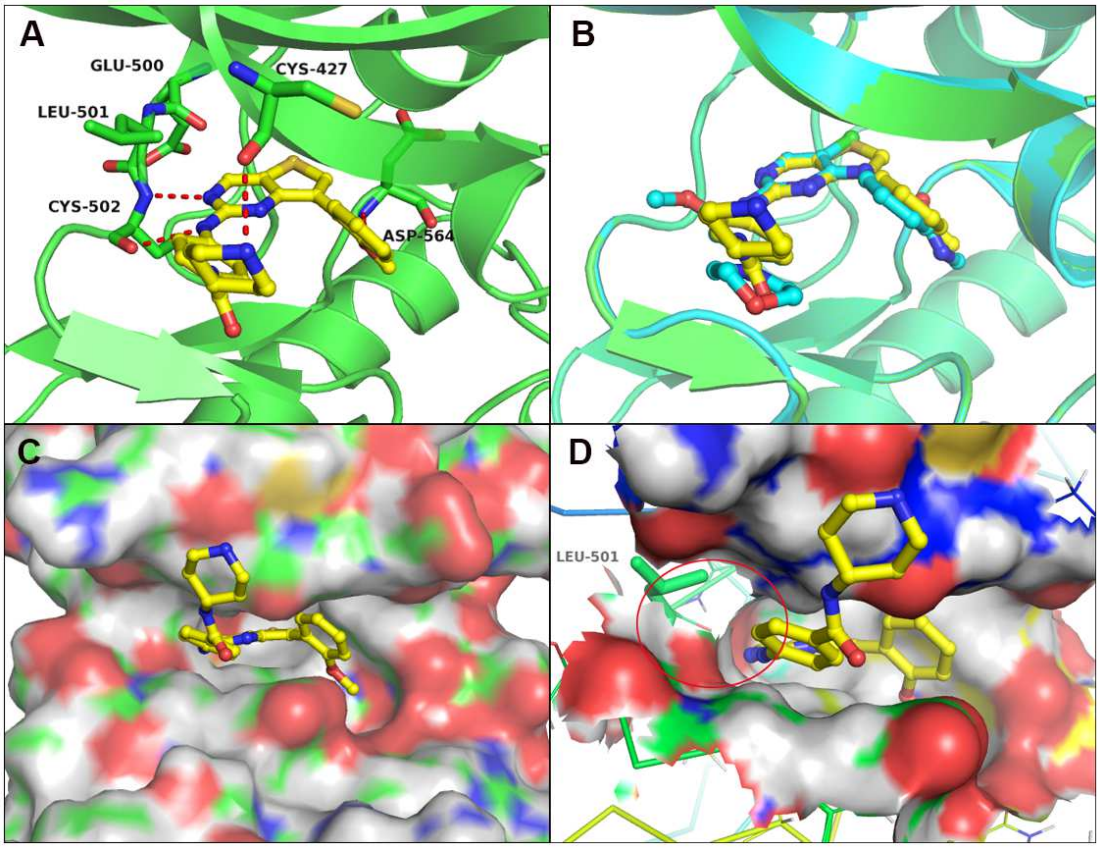

Figure 3. The predicted docked pose of compound **24f** (yellow sticks) in the FAK active site (PDB: 2JKK). (**A**) Detailed interactions with the protein residues. Each dashed red line represents hydrogen bonds. (**B**) Image showing the overlap of compound **24f** and TAE-226 (blue sticks). (**C**) Three-dimensional space matching diagram of compound **24f** and the active site. (**D**) The red frame represents the pocket in the lower hinge area.

Based on the analysis described above, we started the optimization of compound **24f** by varying the substituent on the benzene ring. As shown in **Table 3**, the introduction of F-, Me- or MeO- into R_3 and of F- or Me- into R_4 yielded compounds **26a-c** and **26f-g**, respectively, which retained high potency against FAK, with IC_{50} values ranging from 25.7 to 48.3 nM. Further substitution of the R_3 moiety to larger EtO- (**26d**) and CF_3- (**26e**) groups both resulted in a pronounced loss of activity toward FAK (IC_{50} = 165.6 nM and 709.0 nM, respectively). Clearly, increasing the size of the substituent produced a significant reduction in activity, presumably due to deleterious steric interactions with the amino acid residues of the protein skeleton. The introduction of a fluoro group para to the methoxy substituent or a fluoro substituent on the 2-substituted aniline resulted in the potent inhibitors **26h** (IC_{50} = 38.2 nM) and **26i** (IC_{50} = 24.2 nM).

In cell-based assays, most of the target compounds possessed significant anticancer activities, with IC_{50} values ranging from 0.19 to 3.0 μM. Analogues **26b**, **26f**, **26g** and **26i** exhibited much greater antitumour activities than TAE-226 in U-87MG and MDA-MB-231 cells. More interestingly, the most promising compound, **26f**, displayed stronger potency than TAE-226 in U-87MG, A-549 and MDA-MB-231 cells, with IC_{50} values of 0.16, 0.27, and 0.19 μM, respectively. Furthermore, as shown in **Figure 4,** a significant time- and concentration-dependent decrease was observed in the viability of both A549 and MDA-MB-231 cells after treatment with inhibitor **26f**.

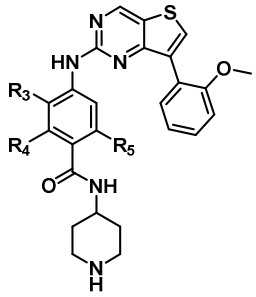

Table 3 Biological activities of compounds **26a-i**.

Compd.	R_3	R_4	R_5	FAK, IC_{50} (nM)[a]	Antiproliferative activity, IC_{50} (μM)[b]		
					U-87MG	A549	MDA-MB-231
24f	H	H	H	38.8	0.65 ± 0.07	0.36 ± 0.06	0.11 ± 0.01
26a	F	H	H	48.3	2.37 ± 0.01	2.75 ± 0.42	1.61 ± 0.33
26b	Me	H	H	26.5	0.25 ± 0.05	3.42 ± 0.17	3.24 ± 0.40
26c	OMe	H	H	27.2	6.40 ± 0.01	2.88 ± 0.28	2.24 ± 0.13
26d	OEt	H	H	165.6	2.03 ± 0.14	5.77 ± 0.14	4.39 ± 0.13
26e	CF_3	H	H	709.0	2.09 ± 0.16	4.11 ± 0.19	2.75 ± 0.18
26f	H	F	H	28.2	0.16 ± 0.02	0.27 ± 0.05	0.19 ± 0.02
26g	H	Me	H	25.7	0.46 ± 0.09	0.87 ± 0.09	0.24 ± 0.04
26h	OMe	H	F	38.2	3.59 ± 0.33	1.90 ± 0.05	1.16 ± 0.05
26i	F	H	F	24.2	1.48 ± 0.25	5.39 ± 0.09	2.57 ± 0.10
TAE-226				6.3	1.67±0.02	1.16±0.20	4.06±0.21

[a] The IC_{50} values are presented as the mean (nM) values from two separate experiments.

[b] Concentration that inhibits the proliferation of cancer cells by 50 %. Cell proliferation was measured using the MTT assay after incubation with the compounds for 72 h. The mean values of three independent experiments ± SE are reported.

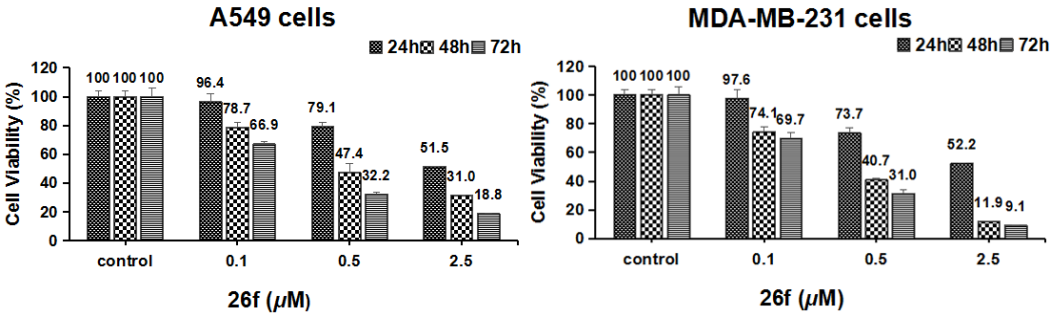

Figure 4. The effects of treatment time and concentration of **26f** on viability of A549 and MDA-MB-231 cells.

At this stage, we had identified compound **26f** as displaying potent enzymatic and cellular activities. We next addressed the effects of variation in the solubilizing group at the R_6 position, the results are reported in **Table 4**. Compared to the piperidine-4-yl-substituted compound **26f**, the tetrahydro-pyran-4-yl analogue **27a** was more than 4-fold less potent, and the 1-methylpiperidine-4-yl analogue **27b** showed a 1.5-fold reduction in potency. Similarly, a lower potency was observed for the pyrrolidin-3-yl analogues **28c-d** and the piperidine-methyl-substituted analogues **28e-g**, indicating that the piperidine-4-yl moiety was an important contributor to the potency of FAK inhibition. In cell-based assays, most compounds possessed moderate anticancer activities, with IC_{50} values less than 5.0 μM. Three of these compounds (**27b**, **28c**, and **28d**) displayed much higher antiproliferative activity than

the others toward the A549 and MDA-MB-231 cell lines, with IC_{50} values in the submicromolar range.

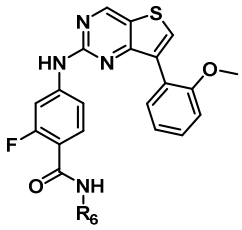

Table 4 Biological activities of compounds **27a-b** and **28c-g**.

Compd.	R_6	FAK, IC_{50} (nM)[a]	Antiproliferative activity, IC_{50} (μM)[b]	
			A549	MDA-MB-231
26f	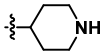	28.2	0.27 ± 0.05	0.19 ± 0.02
27a		117.7	5.71±0.91	5.35±0.01
27b	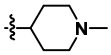	47.8	0.66±0.03	0.35±0.03
28c	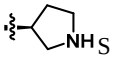	132.3	0.87±0.10	0.56±0.16
28d	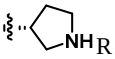	71.3	0.43±0.13	0.26±0.02
28e	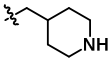	120.2	3.41±0.14	1.53±0.19
28f	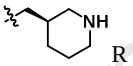	111.2	5.05±0.46	2.89±0.28
28g	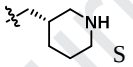	148.9	4.45±0.21	8.62±0.50
TAE-226		6.3	1.16±0.20	4.06±0.21

[a] The IC_{50} values are presented as the mean (nM) values from two separate experiments.

[b] Concentration that inhibits the proliferation of cancer cells by 50 %. Cell proliferation was measured using the MTT assay after incubation with the compounds for 72 h. The mean values of three independent experiments ± SE are reported.

3.2. Cellular selectivity assay

We evaluated the antiproliferative activities of eight compounds toward a normal human cell line, HK2 (normal human tubular epithelial cell line), using the MTT assay to assess the cytotoxicity of the synthesized compounds. These eight compounds potently inhibited enzyme activity and cancer cell proliferation. As shown in **Table 5**, six of these compounds (**24f**, **24g**, **24h**, **26c**, **26f**, and **26g**) displayed low cytotoxicity toward the normal HK2 cells, indicating that these compounds exerted less of an effect on HK2 cells than on the cancer cells. Two compounds (**24e** and **26h**) displayed significant cytotoxicity to HK2 cells, with IC_{50} values < 1.0 μM.

Table 5 Antiproliferative activities of compounds toward HK2 cells

Compd.	HK2 (μM)[a]	Compd.	HK2 (μM)[a]
24e	0.71 ± 0.02	**26c**	12.21 ± 0.11
24f	11.39 ± 1.30	**26f**	3.32 ± 0.20
24g	11.69 ± 0.50	**26g**	4.45 ± 0.22

24h	4.89 ± 0.14	**26h**	0.78 ± 0.04
TAE-226	8.20 ± 1.01		

[a] Concentration that inhibits the proliferation of cancer cells by 50 %. Cell proliferation was measured using the MTT assay after incubation with the compounds for 72 h. The mean values of three independent experiments ± SE are reported.

3.3. Kinase selectivity profile

The kinase selectivity of compound **26f** was profiled against a panel of 25 kinases covering the major tumor progression, metastasis, angiogenesis, oncogenic activation and mitogenic stimulation kinases of the human protein kinome at a concentration of 1.0 μM, and the percent inhibition values are reported in **Table 6**. Compound **26f** is a multi-target kinase inhibitor, with five kinases (ALK, BTK, CDK2, FAK and RET) producing greater than 80% inhibition.

Table 6 Kinase selectivity profile of compound **26f**.[a]

Kinase	%inhibition at 1 μM	kinase	%inhibition at 1 μM	kinase	%inhibition at 1 μM
AKT1	15	IKBKE	66	PAK1	67
ALK	95	IRAK4	72	PIM1	3
BRAF	51	KIT	41	PKA	63
BTK	88	MEK1	27	PRKCQ	48
CAMKK2	77	ERK2	1	FAK	100
CDK2	97	MET	72	RET	97
CHK1	38	MKNK1	13	ROCK1	33
FGFR4	66	mTOR	2	ZAP70	6
HIPK3	72				

[a] Selectivity profile of compound **26f** measured at a concentration of 1 μM in a panel of 25 kinases generated with the SelectScreen® Profiling Service from Life Technologies. The results represent the mean of three independent experiments performed in triplicate.

3.4. Cell apoptosis assay

The apoptosis of MDA-MB-231 cells treated with different concentrations of the optimal derivative **26f** (0.1, 0.2 and 0.4 μM) was analysed by staining cells with Annexin V-FITC and PI and performing flow cytometry to explore whether the antiproliferative activity of compound **26f** toward MDA-MB-231 cells was accompanied by an increase in cancer cell apoptosis. As illustrated in **Figure 5**, compound **26f** substantially increased the apoptosis of MDA-MB-231 cells in a concentration-dependent manner, with apoptotic rates of 11.57 %, 23.33 %, and 41.82 % at concentrations of 0.1, 0.2 and 0.4 μM, respectively.

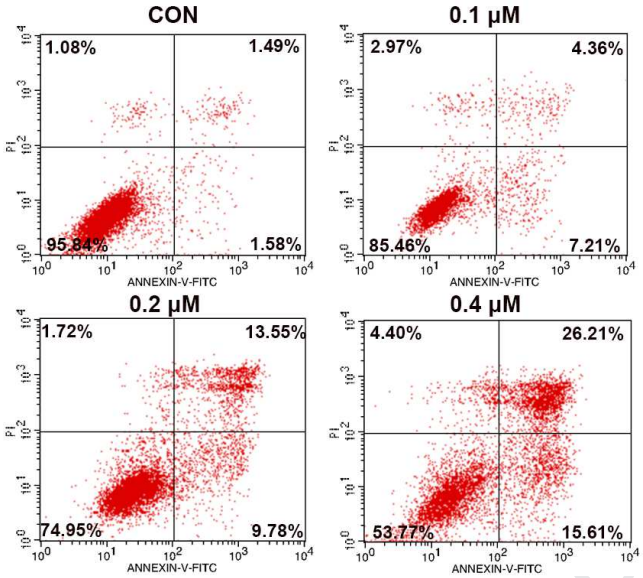

Figure 5. Flow cytometry analyses of apoptosis induction in MDA-MB-231 cells treated with compound **26f** (0.1, 0.2 and 0.4 μM) and untreated cells (control) as a reference control for 48 h. The lower left quadrant represents live cells, the lower right quadrant represents early apoptotic cells, the upper right quadrant represents late apoptotic cells, and the upper left quadrant represents necrotic cells.

3.5. Cell cycle analysis

The effect of compound **26f** on cell cycle progression in MDA-MB-231 cells was analysed using flow cytometry (**Figure 6**). Compared with the control group, the percentages of cells in G0/G1 phase increased from 43.43 % to 56.27 %, whereas the percentage of cells in G2/M phase decreased from 17.40 % to 3.55 % after treatment with 0.1, 0.2 or 0.4 μM compound **26f** for 48 h. The percentage of cells in S phase showed only minor changes. Evidently, derivative **26f** induced the arrest of a significant percentage of cells in G0/G1 phase of the cell cycle compared with untreated cells.

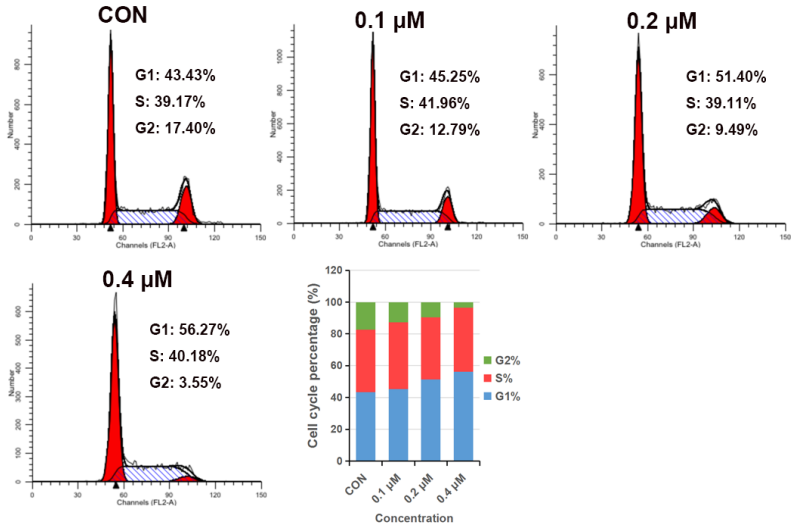

Figure 6. Effects of compound **26f** on the cell cycle of MDA-MB-231 cells. Flow cytometry analysis of the cell cycle in MDA-MB-231 cells treated with compound **26f** (0.1, 0.2 or 0.4 μM) or no treatment (control) for 48 h.

3.6. Cell migration assay

Wound healing assays were performed to investigate the effect of compound **26f** on the migration of

MDA-MB-231 cells. MDA-MB-231 cells were incubated with DMSO or compound **26f** (0.15, 0.3 or 0.6 μM) for 48 h. As illustrated in the photomicrographs shown in **Figure 7**, untreated MDA-MB-231 cells filled most of the wounded area 48 h after scratching the cell monolayer, whereas treatment with the indicated doses of compound **26f** significantly suppressed wound healing in a time- and concentration-dependent manner. These results indicate that compound **26f** possesses a significant ability to inhibit the metastasis of MDA-MB-231 cells.

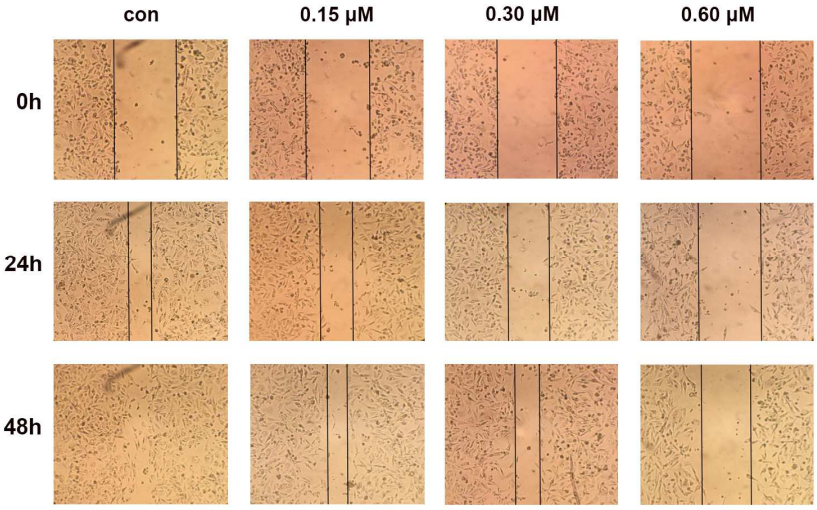

Figure 7. Compound **26f** inhibited the migration of MDA-MB-231 cancer cells in a wound healing assay.

3.7. *In vitro* metabolic stability

We investigated the *in vitro* metabolic stability of compound **26f** in rat liver microsomes. As shown in **Table 7**, compound **26f** was significantly stable in rat liver microsomes ($T_{1/2}$ = 133.8 min).

Table 7 Liver microsomal stability

parameters	$T_{1/2}$ (min)	Remaining (%) T = 1 h	Remaining[a] (%) T = 1 h	$CL_{int(mic)}$ (μL/min/mg)	$CL_{int(liver)}$ (μL/min/mg)
in rat	133.8	72.4	92.1	10.4	18.6

[a] The NADPH regeneration system (replaced with buffer) was not added to the sample during the one hour incubation.

3.8. Molecular docking study

A docking study of compound **26f** in the ATP-binding site of FAK (PDB: 2JKK) was performed to elucidate its interaction mode. The best predicted binding mode is shown in **Figure 8** and has a calculated binding energy of -10.51 kcal/mol. Compound **26f** is anchored to the hinge region *via* the canonical donor-acceptor hydrogen bonding motif between the nitrogen molecules on the 2,7-disubstituted thieno[3,2-*d*]pyrimidine moiety and the backbone of residue Cys502, and further stabilization may be achieved through the hydrophobic interactions of the thieno[3,2-*d*]pyrimidine ring with the hydrophobic side chains of Leu553 and Ala452. Moreover, the bending of the *o*-methoxy moiety back toward the activation loop region results in the formation of a hydrogen bond with Asp564 of the DFG motif. Furthermore, the water-soluble “tail” of the piperidine moiety points toward the solvent by forming a hydrogen bond with Cys427, which is located at the edge of the active pocket, confirming that the piperidine-4-yl moiety is an important contributor to the potency of FAK inhibition. The binding model supported the data obtained from the biological assays described above and provides a structural basis for the further structure-guided design of FAK inhibitors.

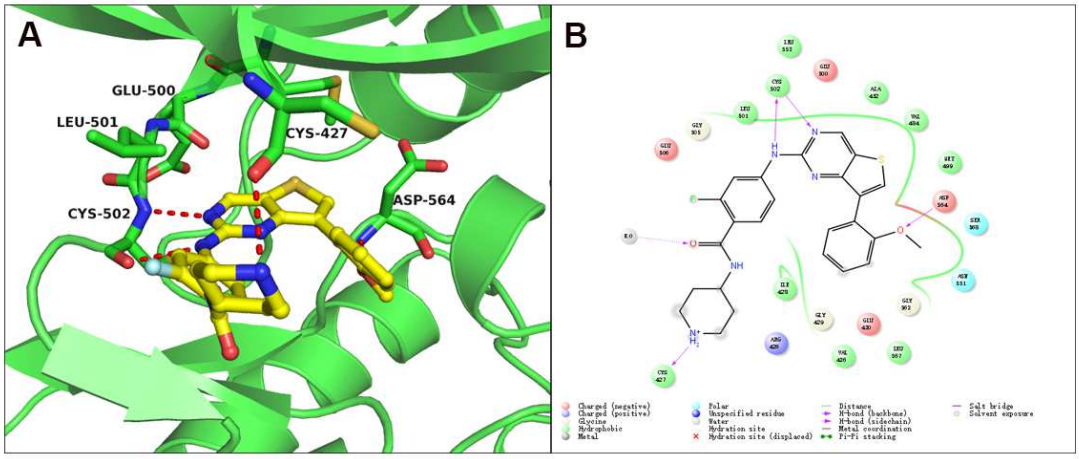

Figure 8. The predicted docked pose of compound **26f** (yellow sticks) in the FAK active site (PDB: 2JKK). (**A**) Detailed interactions with the protein residues. Each dashed red line represents hydrogen bonds. (B) 2D diagram of the interaction between compound **26f** and the active site cavity of FAK.

4. Conclusions

In conclusion, we designed and synthesized a novel 2,7-disubstituted-thieno[3,2-*d*]pyrimidine scaffold as a constrained diaminopyrimidine pharmacophore mimic. Importantly, we validated this scaffold as a new kinase inhibitor platform for designing FAK inhibitors. The structure-activity relationships of these compounds are discussed in this paper from the perspective of enzymatic and cellular activities. Most compounds potently suppressed the enzymatic activities of FAK, with IC_{50} values ranging from 10^{-7}–10^{-8} M, and potently inhibited the proliferation of U-87MG, A-549 and MDA-MB-231 cancer cells. In particular, the optimized compound **26f** potently inhibited the enzyme (IC_{50} = 28.2 nM) and displayed stronger potency than TAE-226 against U-87MG, A-549 and MDA-MB-231 cells, with IC_{50} values of 0.16, 0.27, and 0.19 μM, respectively. Furthermore, compound **26f** effectively induced apoptosis and arrest at the G0/G1 phase of the cell cycle in MDA-MB-231 cells and suppressed the migration of MDA-MB-231 cells. A docking study of compound **26f** was performed to elucidate its possible binding modes and to provide a structural basis for the structure-guided design of FAK inhibitors. The findings reveal that 2,7-disubstituted-thieno[3,2-*d*]pyrimidine derivatives represent a new class of FAK inhibitors that warrant further investigation to generate potential anticancer agents.

5. Experimental section

5.1. Chemistry

Starting materials, reagents and solvents were obtained from commercial suppliers and used without further purification unless otherwise indicated. Anhydrous solvents were dried and stored according to standard procedures. All reactions were monitored by thin layer chromatography (TLC) on silica gel plates with fluorescence F-254 and visualized with UV light. Column chromatography was carried out on silica gel (200-300 mesh). ^{1}H NMR and ^{13}C NMR spectral data were recorded in DMSO-d_6, MeOD or $CDCl_3$ on Bruker ARX-600 NMR or Bruker ARX-400 NMR spectrometers with TMS as an internal standard. High-resolution accurate mass spectrometry (HRMS) determinations for all final target compounds were obtained on a Bruker micromass time of flight mass spectrometer equipped with an electrospray ionization (ESI) detector. All melting points were obtained on a Büchi melting point B-540 apparatus and are uncorrected.

*5.1.1. Preparation of 2-chlorothieno[3,2-d]pyrimidine (**8**)*

A solution composed of 2,4-dichlorothieno[3,2-*d*]pyrimidine (1 equiv) and $NaCO_3$ (1 equiv) in EtOH was mixed with 10 % Pd/C (0.1 equiv). The suspension was stirred at 30 °C under an atmosphere of H_2 for 24 h. The reaction mixture was filtered through a Celite pad with EtOAc washes. The filtrate was washed with H_2O and saline, dried over anhydrous Na_2SO_4, and filtered. The filtrate was concentrated to obtain the crude product **8** for the next step. ^{1}H NMR (600 MHz, DMSO-d_6) δ 9.50 (d, *J* = 0.5 Hz, 1H), 8.64 (d, *J* = 5.4 Hz, 1H), 7.63 (dd, *J* = 5.4, 0.6 Hz, 1H). MS (ESI) m/z(%): 170.9 $[M+H]^+$.

*5.1.2. Preparation of 2-chloro-7-iodothieno[3,2-d]pyrimidine (**9**)*

The intermediate **8** (1 equiv) and *N*-iodosuccinimide (3 equiv) were mixed in acetic acid and heated at 80 °C for 24 h. The reaction was then partitioned between water and EtOAc, and the aqueous layer was extracted twice with EtOAc. The combined organic fractions were washed with saline, dried over anhydrous Na_2SO_4, and filtered. The filtrate was concentrated and purified using chromatography to yield the intermediate **9**. ^{1}H NMR (600 MHz, DMSO-d_6) δ 9.49 (s, 1H), 8.85 (s, 1H). MS (ESI) m/z(%): 296.5 $[M+H]^+$.

*5.1.3. General procedure for the synthesis of intermediates **10a-h**.*

Pd(dppf)Cl_2 (0.1 equiv) was added to a solution of compound **9** (1 equiv), the corresponding boric acid or borate (1.1 equiv), and K_2CO_3 (3 equiv) in 1,4-dioxane:H_2O (4:1) under a nitrogen atmosphere. The mixture was purged with nitrogen for 5 min and then heated at 90 °C until the reaction was complete. The mixture was diluted with ethyl acetate, and the organic layer was washed with saline, dried over anhydrous Na_2SO_4 and filtered. The filtrate was concentrated and purified using column chromatography to produce the coupling intermediates **10a-h**.

*5.1.3.1. 2-chloro-7-(2-methoxyphenyl)thieno[3,2-d]pyrimidine (**10a**).* ^{1}H NMR (600 MHz, DMSO-d_6) δ 9.52 (s, 1H), 8.65 (s, 1H), 7.62–7.60 (m, 1H), 7.44 (t, *J* = 7.2 Hz, 1H), 7.19 (d, *J* = 8.3 Hz, 1H), 7.08 (d, *J* = 7.4 Hz, 1H), 3.77 (s, 3H). MS (ESI) m/z(%): 277.1 $[M+H]^+$.

*5.1.3.2. 2-chloro-7-(3-(methylsulfonyl)phenyl)thieno[3,2-d]pyrimidine (**10d**).* ^{1}H NMR (600 MHz, DMSO-d_6) δ 9.61 (s, 1H), 9.07 (s, 1H), 8.54 (t, *J* = 1.5 Hz, 1H), 8.38 (d, *J* = 7.9 Hz, 1H), 7.99 (d, *J* = 8.2 Hz, 1H), 7.84 (t, *J* = 7.8 Hz, 1H), 3.30 (s, 3H). MS (ESI) m/z(%): 324.9 $[M+H]^+$.

*5.1.4. General procedure for the synthesis of compounds **11a-h**.*

Dimethyl (4-aminobenzyl)phosphonate (1.1 equiv), X-phos (0.1 equiv) and Cs_2CO_3 (3.0 equiv) in 1,4-dioxane, and Pd(AcO)$_2$ (0.05 equiv) were added to solutions of compounds **10a-h** (1 equiv) under a nitrogen atmosphere. The mixture was purged with nitrogen for 5 min and then heated at 90 °C until the reaction was complete. The mixture was diluted with ethyl acetate, and the organic layer was washed with saline, dried over anhydrous Na_2SO_4, filtered and concentrated. The residue was purified using column chromatography to afford compounds **11a-h**.

*5.1.4.1. dimethyl (4-((7-(2-methoxyphenyl)thieno[3,2-d]pyrimidin-2-yl)amino)benzyl)phosphonate (**11a**).* White solid; yield: 73%; mp: 139.6–141.2 °C; ^{1}H NMR (600 MHz, DMSO-d_6) δ 9.65 (s, 1H), 9.20 (s, 1H), 8.38 (s, 1H), 7.80 (dd, *J* = 7.5, 1.5 Hz, 1H), 7.77 (d, *J* = 8.3 Hz, 2H), 7.43 (dd, *J* = 11.5, 4.2 Hz, 1H), 7.19 (d, *J* = 8.1 Hz, 1H), 7.12–7.11 (m, 2H), 7.10–7.08 (m, 1H), 3.79 (s, 3H), 3.58 (d, *J* = 10.7 Hz, 6H), 3.17 (d, *J* = 21.1 Hz, 2H). ^{13}C NMR (150 MHz, DMSO-d_6) δ 159.55, 157.55, 156.86, 153.62, 139.42 (d, *J* = 3.5 Hz), 136.10, 131.15, 131.03, 129.60 (d, *J* = 6.5 Hz, 2C), 129.26, 124.04 (d, *J* = 9.1 Hz), 122.19, 121.80, 119.94, 118.39 (d, *J* = 1.9 Hz, 2C), 111.39, 55.47, 52.32 (d, *J* = 6.5 Hz, 2C), 30.39 (d, *J* = 135.2 Hz). HRMS calcd for $C_{22}H_{22}N_3O_4PS$, $[M+Na]^+$, 478.0961; found 478.0946.

*5.1.4.2. dimethyl (4-((7-(2-acetylphenyl)thieno[3,2-d]pyrimidin-2-yl)amino)benzyl)phosphonate (**11b**).* Yellow solid; yield: 68%; mp: 171.8–172.5 □; ^{1}H NMR (600 MHz, DMSO-d_6) δ 9.55 (s, 1H), 9.18 (s, 1H), 8.25 (s, 1H), 7.89 (d, *J* = 7.6 Hz, 1H), 7.66 (t, *J* = 7.3 Hz, 1H), 7.62 (d, *J* = 8.3 Hz, 2H), 7.58 (t, *J* = 7.5 Hz, 1H), 7.54 (d, *J* = 7.4 Hz, 1H), 7.09 (d, *J* = 6.7 Hz, 2H), 3.58 (d, *J* = 10.7 Hz, 6H), 3.16 (d, *J* = 21.1 Hz, 2H), 2.32 (s, 3H). ^{13}C NMR (150 MHz, DMSO-d_6) δ 200.95, 159.00, 157.66, 153.64, 139.92, 139.19 (d, *J* = 3.0 Hz), 135.62, 134.34, 132.03, 131.62, 131.30, 129.65, 129.58 (d, *J* = 6.5 Hz, 2C), 128.12, 124.27 (d, *J* = 9.3 Hz), 121.94, 118.60 (d, *J* = 1.9 Hz, 2C), 52.31 (d, *J* = 6.6 Hz, 2C), 30.40 (d, *J* = 135.1 Hz), 28.63. HRMS calcd for $C_{23}H_{22}N_3O_4PS$, $[M+Na]^+$, 490.0961; found 490.0963.

*5.1.4.3. dimethyl (4-((7-(3-acetylphenyl)thieno[3,2-d]pyrimidin-2-yl)amino)benzyl)phosphonate (**11c**).* Light yellow solid; yield: 59%; mp: 89.2–90.1 □; ^{1}H NMR (600 MHz, DMSO-d_6) δ 9.76 (s, 1H), 9.26 (s, 1H), 8.67 (s, 1H), 8.57 (t, *J* = 1.4 Hz, 1H), 8.31 (d, *J* = 7.8 Hz, 1H), 8.02–8.00 (m, 1H), 7.80 (d, *J* = 8.4 Hz, 2H), 7.68 (t, *J* = 7.7 Hz, 1H), 7.15 (dd, *J* = 8.6, 2.2 Hz, 2H), 3.59 (d, *J* = 10.8 Hz, 6H), 3.18 (d, *J* = 21.1 Hz, 2H), 2.65 (s, 3H). ^{13}C NMR (150 MHz, DMSO-d_6) δ 197.95, 158.25, 157.75, 154.19, 139.17 (d, *J* = 3.4 Hz), 137.15, 135.21, 133.97, 133.28, 132.67, 129.76 (d, *J* = 6.4 Hz, 2C), 128.89, 127.79, 127.38, 124.43 (d, *J* = 9.2 Hz), 122.82, 118.63 (d, *J* = 1.9 Hz, 2C), 52.33 (d, *J* = 6.6 Hz, 2C), 30.44 (d, *J* = 135.2 Hz), 26.88. HRMS calcd for $C_{23}H_{22}N_3O_4PS$, $[M+Na]^+$, 490.0961; found 490.0948.

*5.1.4.4. dimethyl (4-((7-(3-(methylsulfonyl)phenyl)thieno[3,2-d]pyrimidin-2-yl)amino)benzyl)phosphonate (**11d**).* Light yellow solid; yield: 76%; mp: 107.0–108.1 □; ^{1}H NMR (600 MHz, DMSO-d_6) δ 9.76 (s, 1H), 9.27 (s, 1H), 8.75 (s, 1H), 8.50 (s, 1H), 8.46 (d, *J* = 7.8 Hz, 1H), 7.98 (d, *J* = 7.8 Hz, 1H), 7.81 (t, *J* = 7.8 Hz, 1H), 7.77 (d, *J* = 8.3 Hz, 2H), 7.22 (dd, *J* = 8.5, 2.1 Hz, 2H), 3.60 (d, *J* = 10.7 Hz, 6H), 3.29 (s, 3H), 3.19 (d, *J* = 21.2 Hz, 2H). ^{13}C NMR (150 MHz, DMSO-d_6) δ 158.04, 157.82, 154.29, 141.31, 139.02 (d, *J* = 2.6 Hz), 136.09, 134.63, 132.92, 132.32, 129.89 (d, *J* = 6.5 Hz, 2C), 129.59, 125.98, 125.96, 124.51 (d, *J* = 9.2 Hz), 122.83, 118.77 (2C), 52.34 (d, *J* = 6.8 Hz, 2C), 43.56, 30.49 (d, *J* = 135.2 Hz). HRMS calcd for $C_{22}H_{22}N_3O_5PS_2$, $[M+Na]^+$, 526.0631; found 526.0641.

*5.1.4.5. dimethyl(4-((7-(3-(methylcarbamoyl)phenyl)thieno[3,2-d]pyrimidin-2-yl)amino)benzyl)phosphonate (**11e**).* Light yellow solid; yield: 83%; mp: 98.3–99.0 □; ^{1}H NMR (600 MHz, DMSO-d_6) δ 9.75 (s, 1H), 9.25 (s, 1H), 8.61 (s, 1H), 8.54 (q, *J* = 4.1 Hz, 1H), 8.46 (s, 1H), 8.21 (d, *J* = 7.8 Hz, 1H), 7.86 (d, *J* = 7.8 Hz, 1H), 7.81 (d, *J* = 8.4 Hz, 2H), 7.60 (t, *J* = 7.7 Hz, 1H), 7.15 (dd, *J* = 8.6, 2.2 Hz, 2H), 3.59 (d, *J* = 10.7 Hz, 6H), 3.17 (d, *J* = 21.1 Hz, 2H), 2.84 (d, *J* = 4.5 Hz, 3H). ^{13}C NMR (150 MHz, DMSO-d_6) δ 166.67, 158.29, 157.70, 154.14, 139.15 (d, *J* = 2.9 Hz), 135.01, 134.79, 133.67, 133.52, 130.51, 129.72 (d, *J* = 6.5 Hz, 2C), 128.40, 126.88, 126.34, 124.30 (d, *J* = 9.2 Hz), 122.81, 118.68 (d, *J* = 1.9 Hz, 2C), 52.32 (d, *J* = 6.5 Hz, 2C), 30.54 (d, *J* = 135.3 Hz), 26.31. HRMS calcd for $C_{23}H_{23}N_4O_4PS$, $[M+Na]^+$, 505.1070; found 505.1065.

*5.1.4.6. dimethyl (4-((7-(3-acetamidophenyl)thieno[3,2-d]pyrimidin-2-yl)amino)benzyl)phosphonate (**11f**).* Light yellow solid; yield: 56%; mp: 188.7–190.9 □; ^{1}H NMR (600 MHz, DMSO-d_6) δ 10.07 (s, 1H), 9.72 (s, 1H), 9.23 (s, 1H), 8.44 (s, 1H), 8.17 (s, 1H), 7.83 (d, *J* = 8.3 Hz, 2H), 7.67 (d, *J* = 7.7 Hz, 1H), 7.64 (d, *J* = 8.1 Hz, 1H), 7.43 (d, *J* = 7.9 Hz, 1H), 7.15 (dd, *J* = 8.5, 2.0 Hz, 2H), 3.59 (d, *J* = 10.7 Hz, 6H), 3.18 (d, *J* = 21.1 Hz, 2H), 2.11 (s, 3H). ^{13}C NMR (150 MHz, DMSO-d_6) δ 168.40, 158.36, 157.65, 154.05, 139.45, 139.21 (d, *J* = 2.7 Hz), 134.39, 134.33, 133.93, 129.66 (d, *J* = 6.4 Hz, 2C), 128.66, 124.23 (d, *J* = 9.2 Hz), 123.07, 122.84, 119.06, 118.66 (d, *J* = 1.9 Hz, 2C), 118.63, 52.32 (d, *J* = 6.5 Hz, 2C), 30.50 (d, *J* = 135.4 Hz), 24.02. HRMS calcd for $C_{23}H_{23}N_4O_4PS$, $[M+Na]^+$, 505.1070; found 505.1081.

5.1.4.7.

*Dimethyl (4-((7-(3-(N-methylmethylsulfonamido)phenyl)thieno[3,2-d]pyrimidin-2-yl)amino)benzyl)phosphonate (**11g**).* Yellow solid; yield: 53%; mp: 185.9–186.5 □; ^{1}H NMR (600 MHz, DMSO-d_6) δ 9.73 (s, 1H), 9.24 (s, 1H), 8.62 (s, 1H), 8.07 (d, *J* = 7.8 Hz, 1H), 8.04–8.02 (m, 1H), 7.79 (d, *J* = 8.3 Hz, 2H), 7.56 (t, *J* = 7.9 Hz, 1H), 7.48 (dd, *J* = 8.0, 1.2 Hz, 1H), 7.20 (dd, *J* = 8.6, 2.2 Hz, 2H), 3.60 (d, *J* = 10.8 Hz, 6H), 3.33 (s, 3H), 3.20 (d, *J* = 21.2 Hz, 2H), 2.98 (s, 3H). ^{13}C NMR (150 MHz, DMSO-d_6) δ 158.24, 157.76, 154.19, 142.06, 139.16 (d, *J* = 2.7 Hz), 135.09, 134.43, 133.25, 129.79 (d, *J* = 6.5 Hz, 2C), 129.11, 126.66, 126.04, 125.44, 124.52 (d, *J* = 9.2 Hz), 122.90, 118.79 (d, *J* = 1.9 Hz, 2C), 52.36 (d, *J* = 6.5 Hz, 2C), 37.98, 35.26, 30.45 (d, *J* = 135.3 Hz). HRMS calcd for $C_{23}H_{25}N_4O_5PS_2$, $[M+H]^+$, 533.1077; found 533.1085； $[M+Na]^+$, 555.0896; found 555.0891.

*5.1.4.8. dimethyl (4-((7-(4-methoxyphenyl)thieno[3,2-d]pyrimidin-2-yl)amino)benzyl)phosphonate (**11h**).* Light yellow solid; yield: 78%; mp: 128.2–128.8 ℃; ^{1}H NMR (600 MHz, DMSO-d_6) δ 9.70 (s, 1H), 9.21 (s, 1H), 8.45 (s, 1H), 8.07–8.06 (m, 2H), 7.81 (d, *J* = 8.3 Hz, 2H), 7.22–7.20 (m, 2H), 7.08–7.06 (m, 2H), 3.84 (s, 3H), 3.60 (d, *J* = 10.7 Hz, 6H), 3.21 (d, *J* = 21.2 Hz, 2H). ^{13}C NMR (150 MHz, DMSO-d_6) δ 158.92, 158.41, 157.63, 153.95, 139.26 (d, *J* = 3.3 Hz), 133.66, 132.62, 129.70 (d, *J* = 6.5 Hz, 2C), 129.14 (2C), 126.06, 124.41 (d, *J* = 9.2 Hz), 122.83, 118.80 (d, *J* = 1.8 Hz, 2C), 113.80 (2C), 55.21, 52.32 (d, *J* = 6.5 Hz, 2C), 30.41 (d, *J* = 135.2 Hz). HRMS calcd for $C_{22}H_{22}N_3O_4PS$, $[M+Na]^+$, 478.0961; found 478.0954.

*5.1.5. Preparation of N-(3-(4,4,5,5-tetramethyl-1,3,2-dioxaborolan-2-yl)phenyl)acetamide (**14**)*

Triethylamine (1.2 equiv) and acetic anhydride (1.5 equiv) in CH_2Cl_2 were added to a solution of 3-bromoaniline (1 equiv). The reaction mixture was stirred at rt. Upon completion, the mixture was diluted with water and extracted with CH_2Cl_2. The organic phases were combined, washed with saline, dried over anhydrous Na_2SO_4 and evaporated to afford crude product **13**. Pd(dppf)Cl_2 (0.05 equiv) was added to a solution of compound **13** (1 equiv), bis(pinacolato)diboron (1.2 equiv), and AcOK (3 equiv) in dioxane. The mixture was degassed with nitrogen and heated at 80 °C overnight. The mixture was diluted with ethyl acetate, and the organic layer was washed with saline, dried over anhydrous Na_2SO_4 and filtered. The filtrate was concentrated and purified using chromatography to provide the coupling intermediate **14**. MS (ESI) m/z(%): 262.1 $[M+H]^+$.

*5.1.6.Preparation of N-methyl-N-(3-(4,4,5,5-tetramethyl-1,3,2-dioxaborolan-2-yl)phenyl)methanesulfonamide (**17**)*

Pyridine (2 equiv) was added to a solution of 3-bromoaniline (1 equiv) in CH_2Cl_2 at 0 °C; methanesulfonyl chloride (1 equiv) was then added in a dropwise manner. After 3 h, 1 M HCl was added, and the mixture was diluted with CH_2Cl_2. The organic phases were combined, washed with saline, dried over anhydrous Na_2SO_4 and evaporated to afford crude product **15**. Intermediate **15** (1 equiv) and K_2CO_3 (3 equiv) were dissolved in DMF, and iodomethane (1.1 equiv) was then added in a dropwise manner at rt. After 2 h, water was added in a dropwise manner, and the solution was extracted with CH_2Cl_2. The organic extracts were dried and concentrated in vacuo. The extract was purified using chromatography to produce the intermediate **16**, after which treatment with bis(pinacolato)diboron and Pd(dppf)Cl_2 provided the Suzuki coupling partner intermediate **17**. MS (ESI) m/z(%): 312.2 $[M+H]^+$.

*5.1.7. Preparation of N-methyl-3-(4,4,5,5-tetramethyl-1,3,2-dioxaborolan-2-yl)benzamide (**20**)*

Oxalyl chloride (3 equiv) was added to a solution of 3-bromobenzoic acid (1 equiv) in CH_2Cl_2, to which a catalytic amount of DMF (2 drops) was added. After being stirred at 60 °C for 4 h, the reaction mixture was concentrated and dried under a vacuum. A suspension of CH_3NH_2•HCl (1.5 equiv) and Et_3N (1.5 equiv) in

anhydrous CH_2Cl_2 was then added. The mixture was stirred at 25 °C for 4 h. The mixture was diluted with CH_2Cl_2, and the organic layer was washed with saline, dried over anhydrous Na_2SO_4 and filtered. The filtrate was concentrated and purified using chromatography to yield the intermediate **19**, after which treatment with bis(pinacolato)diboron and Pd(dppf)Cl_2 provided the Suzuki coupling partner intermediate **20**. MS (ESI) m/z(%): 262.1 $[M+H]^+$.

*5.1.8. Preparation of dimethyl (4-aminobenzyl)phosphonate (**23**)*

To a solution of 1-(chloromethyl)-4-nitrobenzene (1 equiv) in trimethyl phosphite (1.5 equiv). The reaction mixture was stirred at 120 ℃ for 10 h. Upon completion, the mixture was diluted with water and extracted with CH_2Cl_2. The organic phases were combined, washed with saline, dried over anhydrous Na_2SO_4 and evaporated to afford crude product **22**. Intermediate **22** (1 equiv) was dissolved in ethanol, and Pd/C (0.1 equiv) was added. The flask was flushed with H_2 and stirred for 3 h at 40 °C. The reaction mixture was filtered through a Celite pad; the filtrate was concentrated and purified using chromatography to produce intermediate **23**. ^{1}H NMR (600 MHz, DMSO-d_6) δ 6.91 (dd, *J* = 8.4, 2.2 Hz, 2H), 6.50 (d, *J* = 8.2 Hz, 2H), 4.98 (s, 2H), 3.56 (d, *J* = 10.7 Hz, 6H), 3.02 (d, *J* = 20.6 Hz, 2H). MS (ESI) m/z(%): 216.0 $[M+H]^+$.

*5.1.9. Preparation of compounds **24a-j**, **26a-i**, **27a-b** and **28c-g**.*

Compounds **24a-j**, **26a-i**, **27a-b** and **28c-g** were prepared in a similar manner as compounds **11a-h**.

*5.1.9.1. diethyl (4-((7-(2-methoxyphenyl)thieno[3,2-d]pyrimidin-2-yl)amino)benzyl)phosphonate (**24a**).* White solid; yield: 67%; mp: 141.2–142.1 □; ^{1}H NMR (600 MHz, DMSO-d_6) δ 9.67 (s, 1H), 9.20 (s, 1H), 8.37 (s, 1H), 7.79 (d, *J* = 6.7 Hz, 3H), 7.41 (t, *J* = 7.6 Hz, 1H), 7.17 (d, *J* = 8.3 Hz, 1H), 7.13 (d, *J* = 7.6 Hz, 2H), 7.09 (t, *J* = 7.4 Hz, 1H), 3.95–3.91 (m, 4H), 3.79 (s, 3H), 3.13 (d, *J* = 21.1 Hz, 2H), 1.17 (t, *J* = 7.0 Hz, 6H). ^{13}C NMR (150 MHz, DMSO-d_6) δ 159.54, 157.54, 156.87, 153.63, 139.37 (d, *J* = 3.3 Hz), 136.08, 131.16, 131.07, 129.64 (d, *J* = 6.4 Hz, 2C), 129.25, 124.27 (d, *J* = 9.2 Hz), 122.20, 121.78, 119.92, 118.22 (2C), 111.36, 61.28 (d, *J* = 6.5 Hz, 2C), 55.46, 31.53 (d, *J* = 135.7 Hz), 16.25 (d, *J* = 5.3 Hz, 2C). HRMS calcd for $C_{24}H_{26}N_3O_4PS$, $[M+Na]^+$, 506.1274; found 506.1259.

*5.1.9.2. ethyl P-(4-((7-(2-methoxyphenyl)thieno[3,2-d]pyrimidin-2-yl)amino)benzyl)-N-methylphosphonamidate (**24b**).* White solid; yield: 58%; mp: 116.7–117.4 □; ^{1}H NMR (600 MHz, DMSO-d_6) δ 9.63 (s, 1H), 9.19 (s, 1H), 8.37 (s, 1H), 7.81 (d, *J* = 7.3 Hz, 1H), 7.76 (d, *J* = 6.6 Hz, 2H), 7.42 (t, *J* = 7.7 Hz, 1H), 7.18 (d, *J* = 8.3 Hz, 1H), 7.12–7.08 (m, 3H), 4.34 (s, 1H), 3.88–3.83 (m, 2H), 3.79 (s, 3H), 2.97 (dd, *J* = 19.6, 4.6 Hz, 2H), 2.38 (dd, *J* = 11.3, 4.8 Hz, 3H), 1.19 (t, *J* = 7.0 Hz, 3H). ^{13}C NMR (150 MHz, DMSO-d_6) δ 159.56, 157.58, 156.85, 153.58, 139.04 (d, *J* = 2.6 Hz), 136.04, 131.14, 131.00, 129.61 (d, *J* = 6.1 Hz, 2C), 129.23, 125.60 (d, *J* = 8.0 Hz), 122.19, 121.68, 119.92, 118.18 (d, *J* = 1.7 Hz, 2C), 111.37, 58.70 (d, *J* = 6.5 Hz), 55.47, 32.81 (d, *J* = 123.7 Hz), 26.67, 16.36 (d, *J* = 6.1 Hz). HRMS calcd for $C_{23}H_{25}N_4O_3PS$, $[M+Na]^+$, 491.1277; found 491.1275.

*5.1.9.3. diethyl (hydroxy(4-((7-(2-methoxyphenyl)thieno[3,2-d]pyrimidin-2-yl)amino)phenyl)methyl)phosphonate (**24c**).* White solid; yield: 43%; mp: 143.2–144.1 □; ^{1}H NMR (600 MHz, DMSO-d_6) δ 9.70 (s, 1H), 9.21 (s, 1H), 8.38 (s, 1H), 7.83–7.78 (m, 3H), 7.45–7.41 (m, 1H), 7.26 (d, *J* = 7.1 Hz, 2H), 7.19 (d, *J* = 8.2 Hz, 1H), 7.09 (t, *J* = 7.4 Hz, 1H), 6.04 (dd, *J* = 16.0, 5.7 Hz, 1H), 4.83 (dd, *J* = 12.4, 5.7 Hz, 1H), 3.98–3.85 (m, 4H), 3.79 (s, 3H), 1.19 (d, *J* = 7.1 Hz, 3H), 1.14 (d, *J* = 7.1 Hz, 3H). ^{13}C NMR (150 MHz, DMSO-d_6) δ 159.51, 157.50, 156.86, 153.63, 140.24 (d, *J* = 2.2 Hz), 136.09, 131.14, 131.10, 130.60, 129.27 (2C), 127.53 (d, *J* = 6.0 Hz), 122.20, 121.85, 119.91, 117.62 (2C), 111.36, 69.09 (d, *J* = 163.9 Hz), 61.89 (dd, *J* = 48.2, 6.6 Hz, 2C), 55.45, 16.33 (dd, *J* = 14.3, 5.2 Hz, 2C). HRMS calcd for $C_{24}H_{26}N_3O_5PS$, $[M+Na]^+$, 522.1223; found 522.1227.

*5.1.9.4. ethyl (4-((7-(2-methoxyphenyl)thieno[3,2-d]pyrimidin-2-yl)amino)benzyl)(morpholino)phosphinate (**24d**).* White solid; yield: 36%; mp: 108.7–109.5 □; ^{1}H NMR (600 MHz, DMSO-d_6) δ 9.66 (s, 1H), 9.19 (s, 1H), 8.37 (s, 1H), 7.80 (t, *J* = 7.6 Hz, 3H), 7.42 (t, *J* = 7.2 Hz, 1H), 7.17 (d, *J* = 8.3 Hz, 1H), 7.13 (d, *J* = 6.9 Hz, 2H), 7.09 (t, *J* = 7.4 Hz, 1H), 3.93–3.85 (m, 2H), 3.79 (s, 3H), 3.46–3.42 (m, 2H), 3.09–3.03 (m, 2H), 2.97–2.93 (m, 2H), 2.86–2.82 (m, 2H), 1.22 (d, *J* = 7.0 Hz, 3H). ^{13}C NMR (150 MHz, DMSO-d_6) δ 159.56, 157.58, 156.88, 153.63, 139.31 (d, *J* = 2.7 Hz), 136.08, 131.17, 131.08, 129.79 (d, *J* = 6.2 Hz, 2C), 129.28, 124.82 (d, *J* = 8.3 Hz), 122.22, 121.78, 119.94, 118.14 (2C), 111.37, 66.46 (d, *J* = 4.5 Hz, 2C), 59.09 (d, *J* = 6.9 Hz), 55.48, 43.77 (2C), 31.90 (d, *J* = 125.7 Hz), 16.26 (d, *J* = 6.0 Hz). HRMS calcd for $C_{26}H_{29}N_4O_4PS$, $[M+Na]^+$, 547.1539; found 547.1545.

*5.1.9.5. 4-((7-(2-methoxyphenyl)thieno[3,2-d]pyrimidin-2-yl)amino)-N-methylbenzamide (**24e**).* White solid; yield: 76%; mp: 210.5–211.3 □; ^{1}H NMR (600 MHz, DMSO-d_6) δ 9.98 (s, 1H), 9.26 (s, 1H), 8.40 (s, 1H), 8.25 (d, *J* = 4.4 Hz, 1H), 7.92 (d, *J* = 8.7 Hz, 2H), 7.77 (dd, *J* = 7.4, 1.3 Hz, 1H), 7.72 (d, *J* = 8.7 Hz, 2H), 7.47–7.44 (m, 1H), 7.21 (d, *J* = 8.3 Hz, 1H), 7.13 (t, *J* = 7.4 Hz, 1H), 3.80 (s, 3H), 2.77 (d, *J* = 4.4 Hz, 3H). ^{13}C NMR (150 MHz, DMSO-d_6) δ 166.27, 159.40, 157.20, 156.86, 153.74, 143.43, 136.35, 131.26, 131.14, 129.40, 127.61 (2C), 126.53, 122.46, 122.12, 120.01, 117.14 (2C), 111.39, 55.48, 26.15. HRMS calcd for $C_{21}H_{18}N_4O_2S$, $[M+H]^+$, 391.1223; found 391.1226.

*5.1.9.6. 4-((7-(2-methoxyphenyl)thieno[3,2-d]pyrimidin-2-yl)amino)-N-(piperidin-4-yl)benzamide Hydrochloride (**24f**).* Light yellow solid; yield: 87%; mp: 211.7–212.4 □; ^{1}H NMR (600 MHz, DMSO-d_6) δ 10.00 (s, 1H), 9.27 (s, 1H), 9.11 (s, 2H), 8.42 (s, 1H), 8.34 (d, *J* = 7.4 Hz, 1H), 7.91 (d, *J* = 8.8 Hz, 2H), 7.79–7.76 (m, 3H), 7.47–7.44 (m, 1H), 7.21 (d, *J* = 8.2 Hz, 1H), 7.13 (t, *J* = 7.4 Hz, 1H), 4.06–4.02 (m, 1H), 3.79 (s, 3H), 3.29 (d, *J* = 12.5 Hz, 2H), 2.97 (dd, *J* = 8.0, 3.6 Hz, 2H), 1.95 (d, *J* = 10.9 Hz, 2H), 1.83 (dd, *J* = 18.3, 7.9 Hz, 2H). ^{13}C NMR (150 MHz, DMSO-d_6) δ 165.55, 159.46, 157.03, 156.88, 153.65, 143.58, 136.73, 131.24, 131.12, 129.48, 128.11 (2C), 126.37, 122.54, 122.10, 120.07, 117.05 (2C), 111.47, 55.56, 44.37, 42.16 (2C), 28.24 (2C). HRMS calcd for $C_{25}H_{25}N_5O_2S$, $[M+H]^+$, 460.1802; found 460.1798.

*5.1.9.7. N-(4-((7-(2-methoxyphenyl)thieno[3,2-d]pyrimidin-2-yl)amino)phenyl)piperidine-4-carboxamide (**24g**).* Light yellow solid; yield: 83%; mp: 250.1–251.2 □; ^{1}H NMR (400 MHz, DMSO-d_6) δ 9.68 (s, 1H), 9.57 (s, 1H), 9.17 (s, 1H), 8.36 (s, 1H), 7.80 (d, *J* = 6.8 Hz, 1H), 7.74 (d, *J* = 8.8 Hz, 2H), 7.44 (dd, *J* = 14.4, 8.1 Hz, 3H), 7.18 (d, *J* = 8.3 Hz, 1H), 7.08 (t, *J* = 7.4 Hz, 1H), 3.79 (s, 3H), 2.97 (d, *J* = 11.7 Hz, 2H), 2.46 (d, *J* = 11.9 Hz, 2H), 2.40–2.33 (m, 1H), 1.96 (s, 1H), 1.64 (t, *J* = 11.2 Hz, 2H), 1.50 (dt, *J* = 12.0, 8.7 Hz, 2H). ^{13}C NMR (150 MHz, DMSO-d_6) δ 173.24, 159.55, 157.57, 156.85, 153.57, 136.15, 135.96, 133.13, 131.16, 131.01, 129.24, 122.23, 121.52, 119.89, 119.30 (2C), 118.48 (2C), 111.35, 55.47, 45.67 (2C), 43.65, 29.54 (2C). HRMS calcd for $C_{25}H_{25}N_5O_2S$, $[M+H]^+$, 460.1802; found 460.1805.

*5.1.9.8. (S)-N-(4-((7-(2-methoxyphenyl)thieno[3,2-d]pyrimidin-2-yl)amino)phenyl)piperidine-3-carboxamide (**24h**).* Light yellow solid; yield: 90%; mp: 219.1–220.2 □; ^{1}H NMR (400 MHz, DMSO-d_6) δ 9.78 (s, 1H), 9.57 (s, 1H), 9.17 (s, 1H), 8.35 (s, 1H), 7.80 (d, *J* = 7.4 Hz, 1H), 7.74 (d, *J* = 8.9 Hz, 2H), 7.44 (d, *J* = 9.0 Hz, 3H), 7.18 (d, *J* = 8.2 Hz, 1H), 7.08 (t, *J* = 7.4 Hz, 1H), 3.79 (s, 3H), 2.99 (d, *J* = 11.8 Hz, 1H), 2.84 (d, *J* = 11.6 Hz, 1H), 2.61 (d, *J* = 10.5 Hz, 1H), 2.42–2.33 (m, 2H), 1.85 (d, *J* = 9.2 Hz, 1H), 1.62–1.55 (m, 2H), 1.41–1.35 (m, 1H). ^{13}C NMR (150 MHz, DMSO-d_6) δ 172.51, 159.55, 157.57, 156.85, 153.57, 136.20, 135.97, 133.00, 131.16, 131.01, 129.25, 122.23, 121.53, 119.90, 119.33 (2C), 118.48 (2C), 111.35, 55.48, 49.08, 45.94, 44.26, 27.89, 25.31. HRMS calcd for $C_{25}H_{25}N_5O_2S$, $[M+H]^+$, 460.1802; found 460.1813.

*5.1.9.9. (R)-N-(4-((7-(2-methoxyphenyl)thieno[3,2-d]pyrimidin-2-yl)amino)phenyl)piperidine-3-carboxamide (**24i**).* Light yellow solid; yield: 82%; mp: 220.0–220.8 □; ^{1}H NMR (600 MHz, MeOD) δ 8.97 (s, 1H), 8.23 (s, 1H), 7.87 (dd, *J* = 7.5, 1.6 Hz, 1H), 7.75 (d, *J* = 9.0 Hz, 2H), 7.42–7.36 (m, 3H), 7.13 (d, *J* = 8.1 Hz, 1H), 7.08 (td, *J* = 7.5, 0.9 Hz, 1H), 3.82 (s, 3H), 3.10 (dd, *J* = 12.4, 3.1 Hz, 1H), 2.97 (d, *J* = 12.4 Hz, 1H), 2.84–2.78 (m, 1H), 2.62 (td, *J* = 12.5, 2.7 Hz, 1H), 2.54–2.49 (m, 1H), 2.02–1.97 (m, 1H), 1.78–1.70 (m, 2H), 1.60–1.54 (m, 1H). ^{13}C NMR (150 MHz, MeOD) δ 175.08, 161.46, 159.06, 158.65, 154.13, 138.58, 136.80, 133.50, 133.03, 132.52, 130.27, 123.83, 123.71, 121.83 (2C), 121.21, 120.01 (2C), 112.24, 56.03, 46.71, 45.37, 29.06, 25.97. HRMS calcd for $C_{25}H_{25}N_5O_2S$, $[M+H]^+$, 460.1802; found 460.1810.

*5.1.9.10. 2-amino-N-(4-((7-(2-methoxyphenyl)thieno[3,2-d]pyrimidin-2-yl)amino)phenyl)acetamide (**24j**).* Light yellow solid; yield: 81%; mp: 205.4–206.3 □; ^{1}H NMR (400 MHz, DMSO-d_6) δ 9.60 (s, 1H), 9.17 (s, 1H), 8.36 (s, 1H), 7.81–7.75 (m, 3H), 7.49 (d, *J* = 8.9 Hz, 2H), 7.43 (dd, *J* = 11.2, 4.4 Hz, 1H), 7.18 (d, *J* = 8.2 Hz, 1H), 7.08 (t, *J* = 7.4 Hz, 1H), 3.79 (s, 3H), 3.24 (s, 2H), 1.94 (s, 2H). ^{13}C NMR (150 MHz, DMSO-d_6) δ 171.48, 159.56, 157.57, 156.85, 153.58, 136.37, 135.98, 132.46, 131.16, 131.01, 129.24, 122.21, 121.56, 119.91, 119.28 (2C), 118.65 (2C), 111.35, 55.47, 45.44. HRMS calcd for $C_{21}H_{19}N_5O_2S$, $[M+Na]^+$, 428.1152; found 428.1150.

*5.1.9.11. 3-fluoro-4-((7-(2-methoxyphenyl)thieno[3,2-d]pyrimidin-2-yl)amino)-N-(piperidin-4-yl)benzamide Hydrochloride (**26a**).* White solid; yield: 79%; mp: 222.5–223.3 □; ^{1}H NMR (600 MHz, DMSO-d_6) δ 9.32 (s, 1H), 9.28 (s, 1H), 9.09 (s, 2H), 8.50 (d, *J* = 7.4 Hz, 1H), 8.45 (s, 1H), 8.28 (t, *J* = 8.4 Hz, 1H), 7.79 (dd, *J* = 12.3, 1.9 Hz, 1H), 7.77 (dd, *J* = 7.5, 1.7 Hz, 1H), 7.66 (dd, *J* = 8.5, 1.7 Hz, 1H), 7.43–7.40 (m, 1H), 7.18 (d, *J* = 7.9 Hz, 1H), 7.07 (td, *J* = 7.5, 0.9 Hz, 1H), 4.08–4.02 (m, 1H), 3.79 (s, 3H), 3.30 (d, *J* = 12.7 Hz, 2H), 3.01–2.96 (m, 2H), 1.95 (dd, *J* = 13.4, 2.8 Hz, 2H), 1.86–1.80 (m, 2H). ^{13}C NMR (150 MHz, DMSO-d_6) δ 164.31, 159.52, 156.91, 156.84, 153.71, 152.51 (d, *J* = 245.3 Hz), 137.12, 131.07, 131.00, 130.97, 129.39, 128.42 (d, *J* = 6.2 Hz), 123.53 (d, *J* = 1.9 Hz), 123.13, 121.92, 121.23, 120.05, 114.24 (d, *J* = 21.1 Hz), 111.45, 55.56, 44.52, 42.12 (2C), 28.14 (2C). HRMS calcd for $C_{25}H_{24}FN_5O_2S$, $[M+H]^+$, 478.1708; found 478.1709.

*5.1.9.12. 4-((7-(2-methoxyphenyl)thieno[3,2-d]pyrimidin-2-yl)amino)-3-methyl-N-(piperidin-4-yl)benzamide (**26b**).* Light yellow solid; yield: 82%; mp: 224.6–225.1 □; ^{1}H NMR (400 MHz, DMSO-d_6) δ 9.10 (s, 1H), 8.33 (s, 1H), 7.96 (t, *J* = 9.5 Hz, 2H), 7.81 (dd, *J* = 7.6, 1.7 Hz, 1H), 7.67 (d, *J* = 1.3 Hz, 1H), 7.58 (dd, *J* = 8.5, 1.9 Hz, 1H), 7.37 (dd, *J* = 11.2, 4.5 Hz, 1H), 7.14 (d, *J* = 8.1 Hz, 1H), 7.02 (td, *J* = 7.5, 0.8 Hz, 1H), 3.83–3.78 (m, 4H), 2.95 (d, *J* = 11.6 Hz, 2H), 2.48–2.45 (m, 2H), 2.29 (s, 3H), 1.72 (dd, *J* = 11.7, 2.1 Hz, 2H), 1.46–1.35 (m, 2H). ^{13}C NMR (150 MHz, DMSO-d_6) δ 165.54, 159.73, 156.84, 156.60, 152.82, 140.57, 138.49, 131.07, 130.90, 129.49, 129.44, 129.07, 128.79, 125.37, 122.28, 121.76, 121.50, 120.06, 111.46, 55.57, 44.42, 42.15 (2C), 28.21 (2C), 18.19. HRMS calcd for $C_{26}H_{27}N_5O_2S$, $[M+H]^+$, 474.1958; found 474.1958.

*5.1.9.13. 3-methoxy-4-((7-(2-methoxyphenyl)thieno[3,2-d]pyrimidin-2-yl)amino)-N-(piperidin-4-yl)benzamide (**26c**).* Yellow solid; yield: 86%; mp: 109.1–111.0 □; ^{1}H NMR (600 MHz, DMSO-d_6) δ 9.26 (s, 1H), 8.53 (d, *J* = 8.4 Hz, 1H), 8.44 (s, 1H), 8.15 (s, 1H), 8.13 (d, *J* = 7.9 Hz, 1H), 7.79 (dd, *J* = 7.5, 1.3 Hz, 1H), 7.51 (s, 1H), 7.48–7.44 (m, 1H), 7.42 (dd, *J* = 8.5, 1.3 Hz, 1H), 7.21 (d, *J* = 8.3 Hz, 1H), 7.13 (t, *J* = 7.4 Hz, 1H), 3.95 (s, 3H), 3.86–3.77 (m, 4H), 2.96 (d, *J* = 12.1 Hz, 2H), 2.51–2.48 (m, 2H), 1.73 (d, *J* = 9.8 Hz, 2H), 1.46–1.40 (m, 2H). ^{13}C NMR (150 MHz, DMSO-d_6) δ 164.85, 159.37, 156.82, 156.71, 153.96, 147.00, 136.80, 131.63, 131.10, 131.06, 129.65, 129.46, 127.47, 122.97, 121.96, 120.05, 116.48, 111.46, 109.28, 56.09, 55.53, 47.44, 45.46 (2C), 33.16 (2C). HRMS calcd for $C_{26}H_{27}N_5O_3S$, $[M+H]^+$, 490.1907; found 490.1911.

*5.1.9.14. 3-ethoxy-4-((7-(2-methoxyphenyl)thieno[3,2-d]pyrimidin-2-yl)amino)-N-(piperidin-4-yl)benzamide (**26d**).* Light yellow solid; yield: 78%; mp: 200.9–201.7 □; ^{1}H NMR (600 MHz, DMSO-d_6) δ 9.27 (s, 1H), 8.55 (d, *J* = 8.4 Hz, 1H), 8.45 (s, 1H), 8.12–8.09 (m, 2H), 7.79 (dd, *J* = 7.5, 1.6 Hz, 1H), 7.50 (d, *J* = 1.4 Hz, 1H), 7.48–7.45 (m, 1H), 7.41 (dd, *J* = 8.5, 1.4 Hz, 1H), 7.22 (d, *J* = 8.2 Hz, 1H), 7.14 (t, *J* = 7.4 Hz, 1H), 4.20 (q, *J* = 6.9 Hz, 2H), 3.83–3.80 (m, 4H), 2.96 (d, *J* = 11.3 Hz, 2H), 2.50–2.46 (m, 2H), 1.73 (d, *J* = 10.7 Hz, 2H), 1.47–1.41 (m, 5H). ^{13}C NMR (100 MHz, DMSO-d_6) δ 164.79, 159.32, 156.81, 156.60, 153.92, 146.04, 136.75, 131.67, 131.49, 131.11, 131.03, 129.44, 127.36, 122.96, 121.95, 120.02, 116.30, 111.46, 110.08, 64.30, 55.50, 47.47, 45.48 (2C), 33.19 (2C), 14.60. HRMS calcd for $C_{27}H_{29}N_5O_3S$, $[M+H]^+$, 504.2064; found 504.2064.

5.1.9.15.
*4-((7-(2-methoxyphenyl)thieno[3,2-d]pyrimidin-2-yl)amino)-N-(piperidin-4-yl)-3-(trifluoromethyl)benzamide (**26e**).* Light yellow solid; yield: 84%; mp: 99.3–100.5 □; ^{1}H NMR (400 MHz, $CDCl_3$) δ 8.95 (s, 1H), 8.89 (d, *J* = 8.7 Hz, 1H), 8.19 (s, 1H), 8.01 (s, 1H), 7.86 (t, *J* = 8.0 Hz, 2H), 7.72 (s, 1H), 7.38 (t, *J* = 7.5 Hz, 1H), 7.11–7.01 (m, 2H), 6.36 (d, *J* = 7.4 Hz, 1H), 4.08–4.02 (m, 1H), 3.81 (s, 3H), 3.08 (d, *J* = 12.0 Hz, 2H), 2.69 (d, *J* = 11.5 Hz, 2H), 2.00 (d, *J* = 10.8 Hz, 2H), 1.47–1.40 (m, 2H). ^{13}C NMR (150 MHz, DMSO-d_6) δ 163.71, 159.50, 157.67, 156.82, 154.00, 140.25, 137.03, 131.72, 131.48, 131.05, 130.86, 129.50, 129.29, 125.52, 125.31, 123.94 (q, *J* = 273.3 Hz), 123.39, 121.89, 120.01, 111.47, 55.54, 47.01, 44.70 (2C), 31.97 (2C). HRMS calcd for $C_{26}H_{24}F_3N_5O_2S$, $[M+H]^+$, 528.1676; found 528.1685.

*5.1.9.16. 2-fluoro-4-((7-(2-methoxyphenyl)thieno[3,2-d]pyrimidin-2-yl)amino)-N-(piperidin-4-yl)benzamide (**26f**).* Light yellow solid; yield: 88%; mp: 131.0–132.1 □; ^{1}H NMR (400 MHz, DMSO-d_6) δ 10.17 (s, 1H), 9.28 (s, 1H), 8.41 (s, 1H), 8.09 (d, *J* = 13.8 Hz, 1H), 7.80 (dd, *J* = 7.7, 3.1 Hz, 1H), 7.74 (dd, *J* = 7.5, 1.7 Hz, 1H), 7.51–7.42 (m, 3H), 7.19 (d, *J* = 8.2 Hz, 1H), 7.11 (td, *J* = 7.5, 0.7 Hz, 1H), 3.81–3.77 (m, 4H), 2.94 (d, *J* = 12.0 Hz, 2H), 2.53–2.47 (m, 2H), 1.77–1.72 (m, 2H), 1.43–1.35 (m, 2H). ^{13}C NMR (100 MHz, DMSO-d_6) δ 162.67 (d, *J* = 1.6 Hz), 159.78 (d, *J* = 245.2 Hz), 159.25, 156.92, 156.81, 153.83, 144.42 (d, *J* = 12.2 Hz), 136.53, 131.41, 131.00, 130.16 (d, *J* = 4.4 Hz), 129.44, 122.90, 122.07, 120.10, 115.61 (d, *J* = 14.2 Hz), 113.51, 111.41, 104.41 (d, *J* = 29.4 Hz), 55.41, 47.25, 45.11 (2C), 32.83 (2C). HRMS calcd for $C_{25}H_{24}FN_5O_2S$, $[M+H]^+$, 478.1708; found 478.1716.

*5.1.9.17. 4-((7-(2-methoxyphenyl)thieno[3,2-d]pyrimidin-2-yl)amino)-2-methyl-N-(piperidin-4-yl)benzamide (**26g**).* Light yellow solid; yield: 83%; mp: 193.0–193.8 □; ^{1}H NMR (400 MHz, $CDCl_3$) δ 8.93 (s, 1H), 8.19 (s, 1H), 7.97 (d, *J* = 7.3 Hz, 1H), 7.69 (s, 1H), 7.47–7.38 (m, 3H), 7.28 (d, *J* = 8.6 Hz, 1H), 7.12 (t, *J* = 7.4 Hz, 1H), 7.06 (d, *J* = 8.3 Hz, 1H), 5.74 (d, *J* = 7.9 Hz, 1H), 4.10–4.01 (m, 1H), 3.84 (s, 3H), 3.12 (d, *J* = 12.2 Hz, 2H), 2.76 (t, *J* = 11.3 Hz, 2H), 2.41 (s, 3H), 2.05 (d, *J* = 10.6 Hz, 2H), 1.42 (d, *J* = 8.8 Hz, 2H). ^{13}C NMR (150 MHz, DMSO-d_6) δ 168.22, 159.44, 157.38, 156.83, 153.70, 141.63, 136.26, 135.82, 131.08, 130.97, 129.66, 129.25, 127.69, 122.23, 122.15, 120.14, 119.48, 114.90, 111.51, 55.50, 45.87, 44.09 (2C), 31.24 (2C), 20.10. HRMS calcd for $C_{26}H_{27}N_5O_2S$, $[M+H]^+$, 474.1958; found 474.1913.

5.1.9.18.
*2-fluoro-5-methoxy-4-((7-(2-methoxyphenyl)thieno[3,2-d]pyrimidin-2-yl)amino)-N-(piperidin-4-yl)benzamide Hydrochloride (**26h**).* Light yellow solid; yield: 87%; mp: 207.9–208.5 □; ^{1}H NMR (400 MHz, DMSO-d_6) δ 9.33 (s, 1H), 9.13–9.03 (m, 2H), 8.48 (t, *J* = 6.7 Hz, 2H), 8.32 (s, 1H), 8.21 (dd, *J* = 7.2, 1.9 Hz, 1H), 7.73 (dd, *J* = 7.5, 1.6 Hz, 1H), 7.49–7.46 (m, 1H), 7.23–7.16 (m, 2H), 7.10 (t, *J* = 7.4 Hz, 1H), 4.05–4.01 (m, 1H), 3.93 (s, 3H), 3.79 (s, 3H), 3.27 (d, *J* = 12.5 Hz, 2H), 2.99 (d, *J* = 11.2 Hz, 2H), 2.02–1.95 (m, 2H), 1.83–1.73 (m, 2H). ^{13}C NMR (150

MHz, DMSO-d_6) δ 163.09, 159.35, 156.77, 155.68, 155.31 (d, *J* = 234.2 Hz), 153.64, 143.30, 137.96, 132.04 (d, *J* = 12.6 Hz), 131.42, 130.97, 129.65, 123.43, 121.81, 120.20, 114.69 (d, *J* = 15.5 Hz), 111.49, 110.51 (d, *J* = 3.8 Hz), 104.88 (d, *J* = 32.4 Hz), 56.54, 55.45, 44.40, 41.95 (2C), 28.03 (2C). HRMS calcd for $C_{26}H_{26}FN_5O_3S$, $[M+H]^+$, 508.1813; found 508.1828.

5.1.9.19. 2,5-difluoro-4-((7-(2-methoxyphenyl)thieno[3,2-d]pyrimidin-2-yl)amino)-N-(piperidin-4-yl)benzamide Hydrochloride ***(26i)***. Light yellow solid; yield: 80%; mp: 235.4–236.6 □; ^{1}H NMR (600 MHz, DMSO-d_6) δ 9.49 (s, 1H), 9.33 (s, 1H), 9.12–9.00 (m, 2H), 8.46 (s, 1H), 8.41 (dd, *J* = 13.0, 6.6 Hz, 1H), 8.35 (d, *J* = 7.1 Hz, 1H), 7.71 (dd, *J* = 7.5, 1.7 Hz, 1H), 7.46–7.41 (m, 2H), 7.18 (d, *J* = 7.9 Hz, 1H), 7.08 (td, *J* = 7.5, 0.8 Hz, 1H), 4.04–3.98 (m, 1H), 3.79 (s, 3H), 3.26 (d, *J* = 12.7 Hz, 2H), 2.98 (q, *J* = 12.0 Hz, 2H), 1.97 (dd, *J* = 13.4, 3.0 Hz, 2H), 1.80–1.73 (m, 2H). ^{13}C NMR (150 MHz, DMSO-d_6) δ 162.22, 159.20, 156.79, 156.49, 155.21 (d, *J* = 243.7 Hz), 153.99, 147.83 (d, *J* = 241.8 Hz), 137.10, 131.59 (t, *J* = 12.5 Hz), 131.42, 131.01, 129.54, 123.65, 121.95, 120.17, 115.95 (dd, *J* = 16.7, 6.0 Hz), 115.37 (dd, *J* = 22.9, 4.3 Hz), 111.44, 107.84 (d, *J* = 31.9 Hz), 55.45, 44.33, 41.89 (2C), 27.93 (2C). HRMS calcd for $C_{25}H_{23}F_2N_5O_2S$, $[M+H]^+$, 496.1613; found 496.1617.

5.1.9.20.

2-fluoro-4-((7-(2-methoxyphenyl)thieno[3,2-d]pyrimidin-2-yl)amino)-N-(tetrahydro-2H-pyran-4-yl)benzamide ***(27a)***. Light yellow solid; yield: 88%; mp: 230.1–231.0 □; ^{1}H NMR (400 MHz, DMSO-d_6) δ 10.16 (s, 1H), 9.28 (s, 1H), 8.41 (s, 1H), 8.09 (d, *J* = 14.4 Hz, 1H), 7.90 (d, *J* = 5.3 Hz, 1H), 7.73 (d, *J* = 7.1 Hz, 1H), 7.53–7.43 (m, 3H), 7.20 (d, *J* = 7.9 Hz, 1H), 7.11 (t, *J* = 7.1 Hz, 1H), 3.97 (s, 1H), 3.86 (d, *J* = 10.4 Hz, 2H), 3.79 (s, 3H), 3.42–3.38 (m, 2H), 1.76 (d, *J* = 11.2 Hz, 2H), 1.58–1.50 (m, 2H). ^{13}C NMR (150 MHz, DMSO-d_6) δ 162.86, 159.80 (d, *J* = 245.8 Hz), 159.26, 156.91, 156.82, 153.86, 144.52 (d, *J* = 12.2 Hz), 136.57, 131.45, 131.01, 130.19 (d, *J* = 4.1 Hz), 129.48, 122.94, 122.08, 120.13, 115.45 (d, *J* = 14.2 Hz), 113.55, 111.44, 104.40 (d, *J* = 29.4 Hz), 66.04 (2C), 55.43, 45.63, 32.34 (2C). HRMS calcd for $C_{25}H_{23}FN_4O_3S$, $[M+Na]^+$, 501.1369; found 501.1362.

5.1.9.21.

2-fluoro-4-((7-(2-methoxyphenyl)thieno[3,2-d]pyrimidin-2-yl)amino)-N-(1-methylpiperidin-4-yl)benzamide ***(27b)***. Yellow solid; yield: 83%; mp: 222.5–223.2 □; ^{1}H NMR (600 MHz, DMSO-d_6) δ 10.17 (s, 1H), 9.29 (s, 1H), 8.41 (s, 1H), 8.09 (d, *J* = 14.1 Hz, 1H), 7.87 (d, *J* = 5.4 Hz, 1H), 7.73 (dd, *J* = 7.4, 1.1 Hz, 1H), 7.51–7.43 (m, 3H), 7.20 (d, *J* = 8.3 Hz, 1H), 7.11 (t, *J* = 7.4 Hz, 1H), 3.79 (s, 3H), 3.76–3.72 (m, 1H), 2.82 (d, *J* = 10.7 Hz, 2H), 2.23 (s, 3H), 2.10 (d, *J* = 9.0 Hz, 2H), 1.79 (d, *J* = 10.7 Hz, 2H), 1.61–1.55 (m, 2H). ^{13}C NMR (150 MHz, DMSO-d_6) δ 163.00, 159.79 (d, *J* = 245.4 Hz), 159.27, 156.92, 156.82, 153.89, 144.50 (d, *J* = 12.4 Hz), 136.61, 131.45, 131.03, 130.18 (d, *J* = 4.0 Hz), 129.49, 122.94, 122.08, 120.13, 115.52 (d, *J* = 14.1 Hz), 113.53, 111.44, 104.40 (d, *J* = 29.2 Hz), 55.44, 54.00 (2C), 45.98, 45.45, 30.93 (2C). HRMS calcd for $C_{26}H_{26}FN_5O_2S$, $[M+H]^+$, 492.1864; found 492.1874.

5.1.9.22. (S)-2-fluoro-4-((7-(2-methoxyphenyl)thieno[3,2-d]pyrimidin-2-yl)amino)-N-(pyrrolidin-3-yl)benzamide ***(28c)***. Light yellow solid; yield: 76%; mp: 162.8–163.6 □; ^{1}H NMR (600 MHz, DMSO-d_6) δ 10.18 (s, 1H), 9.28 (s, 1H), 8.41 (s, 1H), 8.09 (d, *J* = 14.4 Hz, 1H), 7.98 (d, *J* = 4.8 Hz, 1H), 7.73 (d, *J* = 7.2 Hz, 1H), 7.50 (d, *J* = 8.3 Hz, 1H), 7.47–7.44 (m, 2H), 7.20 (d, *J* = 8.3 Hz, 1H), 7.11 (t, *J* = 7.4 Hz, 1H), 4.31–4.27 (m, 1H), 3.79 (s, 3H), 2.97 (dd, *J* = 11.1, 6.6 Hz, 1H), 2.91 (dd, *J* = 11.8, 5.1 Hz, 1H), 2.75 (dd, *J* = 11.5, 5.0 Hz, 1H), 2.66 (dd, *J* = 11.1, 3.8 Hz, 1H), 2.01–1.95 (m, 1H), 1.63–1.60 (m, 1H). ^{13}C NMR (150 MHz, DMSO-d_6) δ 163.30, 159.86 (d, *J* = 245.6 Hz), 159.28, 156.93, 156.84, 153.91, 144.56 (d, *J* = 12.0 Hz), 136.62, 131.48, 131.04, 130.24 (d, *J* = 4.0 Hz), 129.52, 122.97, 122.09, 120.15, 115.37 (d, *J* = 14.2 Hz), 113.56, 111.44, 104.41 (d, *J* = 29.6 Hz), 55.44, 52.89,

50.57, 45.40, 32.61. HRMS calcd for $C_{24}H_{22}FN_5O_2S$, $[M+H]^+$, 464.1551; found 464.1561.

*5.1.9.23. (R)-2-fluoro-4-((7-(2-methoxyphenyl)thieno[3,2-d]pyrimidin-2-yl)amino)-N-(pyrrolidin-3-yl)benzamide (**28d**).* Light yellow solid; yield: 81%; mp: 161.9–162.8 □; ^{1}H NMR (400 MHz, MeOD) δ 9.04 (s, 1H), 8.25 (s, 1H), 8.15 (d, *J* = 15.1 Hz, 1H), 7.79 (d, *J* = 7.2 Hz, 1H), 7.62 (t, *J* = 8.6 Hz, 1H), 7.41–7.34 (m, 2H), 7.18–7.04 (m, 2H), 4.50 (s, 1H), 3.82 (s, 3H), 3.23 (dd, *J* = 11.6, 6.9 Hz, 1H), 3.18–3.10 (m, 1H), 3.04–2.88 (m, 2H), 2.23 (dt, *J* = 14.4, 7.6 Hz, 1H), 1.85 (dd, *J* = 12.0, 5.8 Hz, 1H). ^{13}C NMR (150 MHz, MeOD) δ 166.63 (d, *J* = 1.7 Hz), 162.39 (d, *J* = 245.9 Hz), 161.07, 158.59, 158.32, 154.34, 147.05 (d, *J* = 12.9 Hz), 137.08, 133.39, 132.35, 131.64 (d, *J* = 3.5 Hz), 130.43, 125.04, 123.71, 121.41, 114.93, 114.85, 112.31, 105.87 (d, *J* = 30.4 Hz), 55.99, 53.22, 52.11, 46.33, 33.22. HRMS calcd for $C_{24}H_{22}FN_5O_2S$, $[M+H]^+$, 464.1551; found 464.1560.

*5.1.9.24. 2-fluoro-4-((7-(2-methoxyphenyl)thieno[3,2-d]pyrimidin-2-yl)amino)-N-(piperidin-4-ylmethyl)benzamide (**28e**).* Yellow solid; yield: 91%; mp: 182.5–183.2 □; ^{1}H NMR (600 MHz, DMSO-d_6) δ 9.05 (s, 1H), 8.27 (s, 1H), 7.94 (d, *J* = 16.2 Hz, 1H), 7.87 (d, *J* = 7.4 Hz, 1H), 7.67 (s, 1H), 7.45 (t, *J* = 9.0 Hz, 1H), 7.43–7.39 (m, 1H), 7.30 (d, *J* = 8.6 Hz, 1H), 7.17 (d, *J* = 7.8 Hz, 1H), 7.08 (td, *J* = 7.5, 0.9 Hz, 1H), 3.80 (s, 3H), 3.10 (s, 2H), 2.90 (d, *J* = 12.0 Hz, 2H), 2.39 (t, *J* = 11.3 Hz, 2H), 1.85–1.82 (m, 1H), 1.57 (d, *J* = 10.2 Hz, 2H), 1.01 (qd, *J* = 12.6, 3.7 Hz, 2H). ^{13}C NMR (150 MHz, DMSO-d_6) δ 163.69 (d, *J* = 2.0 Hz), 160.53 (d, *J* = 243.9 Hz), 160.11, 159.87, 156.75, 153.08, 134.87, 131.02, 130.97, 129.74 (d, *J* = 4.3 Hz), 129.01, 122.54, 119.99, 119.79, 116.05, 111.57, 111.32, 104.97 (d, *J* = 27.0 Hz), 55.41, 45.99 (2C), 45.26, 36.54, 31.12 (2C). HRMS calcd for $C_{26}H_{26}FN_5O_2S$, $[M+H]^+$, 492.1864; found 492.1876.

5.1.9.25.
*(R)-2-fluoro-4-((7-(2-methoxyphenyl)thieno[3,2-d]pyrimidin-2-yl)amino)-N-(piperidin-3-ylmethyl)benzamide (**28f**).* Light yellow solid; yield: 82%; mp: 213.1–214.3 □; ^{1}H NMR (600 MHz, $CDCl_3$) δ 8.96 (s, 1H), 8.19 (s, 1H), 8.12 (d, *J* = 15.0 Hz, 1H), 7.97 (t, *J* = 8.8 Hz, 1H), 7.90 (d, *J* = 6.5 Hz, 1H), 7.77 (s, 1H), 7.44 (t, *J* = 7.3 Hz, 1H), 7.17–7.14 (m, 2H), 7.08 (d, *J* = 8.3 Hz, 1H), 6.83–6.78 (m, 1H), 3.84 (s, 3H), 3.42–3.38 (m, 1H), 3.36–3.31 (m, 1H), 3.18 (d, *J* = 11.7 Hz, 1H), 3.07 (d, *J* = 11.9 Hz, 1H), 2.63 (t, *J* = 10.8 Hz, 1H), 2.47 (t, *J* = 11.0 Hz, 1H), 1.91–1.86 (m, 2H), 1.74 (d, *J* = 13.5 Hz, 1H), 1.59–1.53 (m, 1H), 1.23–1.19 (m, 1H). ^{13}C NMR (150 MHz, CD_3Cl) δ 163.78 (d, *J* = 3.4 Hz), 161.60 (d, *J* = 243.7 Hz), 160.09, 157.04, 156.67, 152.89, 144.81 (d, *J* = 13.5 Hz), 135.97, 132.32 (d, *J* = 3.4 Hz), 131.98, 131.41, 129.66, 124.16, 122.02, 120.62, 114.05, 113.24 (d, *J* = 12.3 Hz), 111.27, 104.89 (d, *J* = 32.4 Hz), 55.65, 50.15, 46.49, 43.43, 36.99, 28.83, 25.27. HRMS calcd for $C_{26}H_{26}FN_5O_2S$, $[M+H]^+$, 492.1864; found 492.1876.

5.1.9.26.
*(S)-2-fluoro-4-((7-(2-methoxyphenyl)thieno[3,2-d]pyrimidin-2-yl)amino)-N-(piperidin-3-ylmethyl)benzamide (**28g**).* Light yellow solid; yield: 85%; mp: 214.2–215.0 □; ^{1}H NMR (600 MHz, DMSO-d_6) δ 10.18 (s, 1H), 9.29 (s, 1H), 8.42 (s, 1H), 8.08 (dd, *J* = 14.5, 1.3 Hz, 1H), 7.97 (dd, *J* = 9.1, 5.3 Hz, 1H), 7.73 (dd, *J* = 7.5, 1.6 Hz, 1H), 7.51 (t, *J* = 8.5 Hz, 1H), 7.48–7.43 (m, 2H), 7.20 (d, *J* = 8.2 Hz, 1H), 7.11 (t, *J* = 7.4 Hz, 1H), 3.79 (s, 3H), 3.08 (t, *J* = 6.4 Hz, 2H), 2.90 (d, *J* = 9.6 Hz, 1H), 2.80 (d, *J* = 11.6 Hz, 1H), 2.40 (td, *J* = 11.4, 2.4 Hz, 1H), 2.19–2.15 (m, 1H), 1.74–1.70 (m, 1H), 1.64–1.61 (m, 1H), 1.55 (dd, *J* = 10.6, 4.4 Hz, 1H), 1.31–1.28 (m, 1H), 1.07–1.01 (m, 1H). ^{13}C NMR (150 MHz, DMSO-d_6) δ 163.42, 159.84 (d, *J* = 245.0 Hz), 159.27, 156.93, 156.83, 153.90, 144.52 (d, *J* = 12.3 Hz), 136.62, 131.44, 131.05, 130.27 (d, *J* = 4.3 Hz), 129.48, 122.94, 122.09, 120.13, 115.28 (d, *J* = 14.2 Hz), 113.61, 111.44, 104.41 (d, *J* = 29.4 Hz), 55.44, 50.58, 46.56, 43.04, 36.78, 29.09, 25.71. HRMS calcd for $C_{26}H_{26}FN_5O_2S$, $[M+H]^+$, 492.1864; found 492.1875.

*5.1.10. General procedure for the synthesis of intermediates **31a-f** and **34a-g**.*

HATU (1.2 equiv) and DIEA (1.5 equiv) were added to a solution of 2-fluoro-4-nitrobenzoic acid (1 equiv) and R_6-NH_2 (1 equiv) in CH_2Cl_2 at rt. The resulting mixture was heated to 25–40 °C and stirred until the reaction was complete. The mixture was diluted with ethyl acetate, and the organic layer was washed with saline, dried over anhydrous Na_2SO_4 and filtered. The filtrate was concentrated and purified using chromatography to yield the intermediates **33a-g**. Intermediates **33a-g** (1 equiv) were dissolved in ethanol, and Pd/C (0.1 equiv) was added. The flask was flushed with H_2 and stirred for 6 h at 40 °C. The reaction mixture was filtered through a Celite pad and the filtrate was concentrated to dryness, yielding intermediates **34a-g**.

*5.1.11. Preparation of diethyl (4-aminobenzyl)phosphonate (**36**)*

Intermediate **36** was prepared in a similar manner as intermediate **23**. MS (ESI) m/z(%): 244.0 $[M+H]^+$

*5.1.12. General procedure for the synthesis of intermediates **38** and **40**.*

To a solution of 1-(chloromethyl)-4-nitrobenzene (1 equiv) in triethyl phosphite (1.5 equiv). The reaction mixture was stirred at 130 °C for 10 h. Upon completion, the mixture was diluted with water and extracted with CH_2Cl_2. The organic phases were combined, washed with saline, dried over anhydrous Na_2SO_4 and evaporated to afford crude product **35**. Oxalyl chloride (3 equiv) was added to a solution of compound **35** (1 equiv) in CH_2Cl_2, to which a catalytic amount of DMF (2 drops) was added. The reaction was stirred at 60 °C for 4 h. The reaction mixture was concentrated and dried under a vacuum. A suspension of CH_3NH_2•HCl (1.2 equiv) or morpholine (1.2 equiv) and Et_3N (1.5 equiv) in anhydrous CH_2Cl_2 was then added. The mixture was stirred at 25 °C for 4 h and then diluted with CH_2Cl_2, and the organic layer was washed with saline, dried over anhydrous Na_2SO_4 and filtered. The filtrate was concentrated and purified using chromatography to yield intermediate **37** or **39**. Intermediate **37** or **39** (1 equiv) was dissolved in ethanol, and Pd/C (0.1 equiv) was added. The flask was flushed with H_2 and stirred for 6 h at 40 °C. The reaction mixture was filtered through a Celite pad, and the filtrate was concentrated to dryness, yielding intermediate **38** or **40**. **38**: MS (ESI) m/z(%): 285.1 $[M+H]^+$; **40**: MS (ESI) m/z(%): 229.1 $[M+H]^+$.

5.2. Pharmacological assay

5.2.1. FAK HTRF assay

The FAK kinase assay was performed using the HTRF® KinEASE™-TK kit (Cisbio Bioassays, France) in white 384-well small volume plates with a total working volume of 20 μL. The purified FAK enzyme was purchased from Carna Biosciences (Japan). Compounds were diluted with kinase reaction buffer in a stepwise manner from a concentrated stock of 8 mM in 100 % DMSO. The IC_{50} measurements were performed in replicates. For each assay, 4 μL of dispensed compounds, 4 μL of mix 1 (ATP +Substrate TK) and 2 μL of the kinase (0.111 ng/μL) were added to the assay wells. The assay plates were incubated at 25 °C for 50 min, and reactions were terminated by adding 10 μL of mix 2 (Sa-XL665+TK-Antibody-Cryptate). After a final incubation (60 min at room temperature), HTRF signals were obtained by measuring the fluorescence of the plates at 620 nM (Cryptate) and 665 nM (XL665) using an Infinite® F500 microplate reader (Tecan, Switzerland). A ratio was calculated (665/620) for each well. For IC_{50} measurements, values were normalized and fitted with Prism software (GraphPad software).

5.2.2. Cell proliferation assay

U-87MG, A549, MDA-MB-231 and HK2 cells were cultured in a 96-well plate at a density of 4000–5000 cells/well and were maintained at 37 °C in a humidified atmosphere of 5 % CO_2 for 24 h. The tested compounds

were added to the culture medium at the indicated final concentrations and incubated for 72 h. Fresh MTT was added to each well at a final concentration of 5 mg/mL in phosphate-buffered saline (PBS), and the cells were then incubated at 37 °C for 4 h. The formazan crystals in each well were dissolved in 150 mL DMSO, and the absorbance of each test well was measured at λ_{490nm} using a Thermo reader (Multiskan GO).

5.2.3. Cell apoptosis analysis

The ability of compound **26f** to induce the apoptosis of MDA-MB-231 cells was quantified by performing annexin V and PI staining and flow cytometry. Briefly, after treatment with compound **26f** for 48 h, cells were harvested, washed twice with PBS, and subjected to annexin V and propidium iodide staining using the annexin V FITC apoptosis kit (US Everbright® Inc.) according to the manufacturer's protocol. After staining, flow cytometry (Becton-Dickinson FACSCalibur) was performed to quantify the number of apoptotic cells.

5.2.4. Cell cycle analysis

MDA-MB-231 cells (1×10^6 cells) were seeded in six-well plates and cultured for 24 h. Then, the cells were treated with DMSO or one of several concentrations of compound **26f** for 48 h. After incubation, cells were collected, washed twice with cold PBS and then fixed with ethanol (70 %) at 4 °C overnight. The cells were centrifuged to remove the fixative solution and washed twice with cold PBS. Finally, the cells were stained with PI at 4 °C in the dark for 30 min. The cells were analysed using a flow cytometer with the Cell Quest acquisition and analysis software program (Becton-Dickinson FACSCalibur).

5.2.5. Wound healing assay

MDA-MB-231 cells (2×10^6/well) were seeded in six-well plates and grown to approximately 100 % confluence in culture medium. Subsequently, a cell-free line was manually created by scratching the confluent cell monolayers with a 200 μL pipette tip. The wounded cell monolayers were washed three times with phosphate-buffered saline (PBS) and incubated with serum-free medium. Then, cells were treated with different concentrations of compound **26f**, incubated for 48 h, and photographed at 24 and 48 h with an inverted microscope.

5.2.6. Liver microsomal stability assay

The liver microsomal stability assay was performed by incubating with microsomes (rat microsome, Biopredic, Lot No. MIC254034) (0.5 mg/mL) at 37 °C with compound **26f** at a final concentration of 1 μM in potassium phosphate buffer (pH 7.4, 100 mM with 10 mM $MgCl_2$). The incubation was initiated by the addition of prewarmed cofactors (1 mmol NADPH). After incubation at 37 °C for different times (0, 5, 10, 20, 30, and 60 min), the protein was precipitated by the addition of cold acetonitrile. Then, the precipitated proteins were then removed by centrifugation , and the supernatants were injected into an LC-MS/MS system. The metabolic stability tests of rat livers are fully in accordance with the Guide for the Care and Use of Laboratory Animals.

5.2.7. Molecular docking study

Ligand structures were prepared using Maestro 9.0 within the Schrödinger package. The crystal structures of FAK (PDB ID: 2JKK) were retrieved from the RCSB Protein Data Bank (http://www.pdb.org) and prepared for molecular docking using Protein Preparation Wizard. The ligand structures were optimized with the Maestro Ligprep module, regulated to a protonated state of pH 7.4, and minimized with an OPLS 2005 force field to produce low-energy conformers. Compounds were docked into binding sites with the Glide module within the Schrödinger package using the united-atom scoring function. For all docking simulations, the grid centre was

placed on the centroid of the included ligand binding site, and a 20×20×20 Å grid box size was used. The docking simulation was performed twenty times to provide a sufficient number of constellation groups, and the output was characterized by the favourable binding affinity value. In addition, the figures were prepared using PyMOL.

Acknowledgments

We gratefully acknowledge the financial support from the Program for Innovative Research Team of the Ministry of Education and Program for Liaoning Innovative Research Team in University.

References

[1] M.J. Nimwegen, Van, V.D.W. Bob, Focal adhesion kinase: a potential target in cancer therapy, Biochem. Pharmacol., 73 (2007) 597-609.

[2] H. Baotran, O. Gretchen, F. Sheila, G. Irwin, W.G. Cance, V.M. Golubovskaya, Nanog increases focal adhesion kinase (FAK) promoter activity and expression and directly binds to FAK protein to be phosphorylated, J. Biol. Chem., 287 (2012) 18656-18673.

[3] S. Markus, F. Elaine, Tumor-initiating stem cells of squamous cell carcinomas and their control by TGF-β and integrin/focal adhesion kinase (FAK) signaling, Proc. Natl. Acad. Sci. U. S. A., 108 (2011) 10544-10549.

[4] Z. Xiaofeng, G. Jun-Lin, Focal adhesion kinase and its signaling pathways in cell migration and angiogenesis, Advanced Drug Delivery Reviews, 63 (2011) 610-615.

[5] H. Fan, X. Zhao, S. Sun, M. Luo, J.L. Guan, Function of focal adhesion kinase scaffolding to mediate endophilin A2 phosphorylation promotes epithelial-mesenchymal transition and mammary cancer stem cell activities in vivo, J. Biol. Chem., 288 (2013) 3322-3333.

[6] L. An, W. Li, X. Hu, W. Zhang, S. Zhao, Abundant Focal Adhesion Kinase Causes Aberrant Neuronal Migration Via Its Phosphorylation at Tyr925, J. Mol. Neurosci., 64 (2018) 102-110.

[7] C. Lei, H. Juan, Z. Xianlu, X. Yan, D. Jiahong, L. Xiaowu, Overexpression and significance of focal adhesion kinase in hepatocellular carcinoma and its relationship with HBV infection, Med. Oncol., 26 (2009) 409-414.

[8] A.L. Lark, C.A. Livasy, C. Benjamin, C. Laura, D.T. Moore, Y. Xihui, W.G. Cance, Overexpression of focal adhesion kinase in primary colorectal carcinomas and colorectal liver metastases: immunohistochemistry and real-time PCR analyses, Clin. Cancer Res., 9 (2003) 215-222.

[9] P.L. Judson, X. He, ., W.G. Cance, L. Le, Van, Overexpression of focal adhesion kinase, a protein tyrosine kinase, in ovarian carcinoma, Cancer, 86 (1999) 1551-1556.

[10] L. Yao, K. Li, W. Peng, Q. Lin, S. Li, X. Hu, X. Zheng, Z. Shao, An aberrant spliced transcript of focal adhesion kinase is exclusively expressed in human breast cancer, J. Transl. Med., 12 (2014) 136.

[11] R. Christian, Y. Loïc, B.R. Odile, M.D.M. Véronique, R. Jean-Bernard, C. Pascal, D. Cécile, P. Bernard, L. Guy, R.S. Claire, Expression of focal adhesion kinase in acute myeloid leukemia is associated with enhanced blast migration, increased cellularity, and poor prognosis, Cancer Res., 64 (2004) 3191-3197.

[12] A. Abdulkader, F. Wakkas, J.H. Scholefield, L.G. Durrant, I. Mohammad, Nuclear expression of phosphorylated focal adhesion kinase is associated with poor prognosis in human colorectal cancer, Anticancer Res., 34 (2014) 3969-3974.

[13] H. Jiang, S. Hegde, B.L. Knolhoff, Y. Zhu, J.M. Herndon, M.A. Meyer, T.M. Nywening, W.G. Hawkins, I.M. Shapiro, D.T. Weaver, Targeting focal adhesion kinase renders pancreatic cancers responsive to checkpoint immunotherapy, Nat. Med., 22 (2016) 851-860.

[14] S. Alan, L. Tom, S. Bryan, B. Adam, R.C. Mcpherson, V.K. Alexander, G.C. Laura, C. Marta, M. Morwenna, J.E. Ring, Nuclear FAK Controls Chemokine Transcription, Tregs, and Evasion of Anti-tumor Immunity, Cell, 163 (2015) 160-173.

[15] N. Kurio, T. Shimoa, M. Takaoka, T. Okui, N.M.M. Hassan, T. Honami, S. Hatakeyama, M. Ikeda, Y. Naomoto, A. Sasaki, Anti-tumor effect in human breast cancer by TAE226, a dual inhibitor for FAK and IGF-IR, Exp. Cell Res., 317 (2011) 1134-1146.

[16] M. Roy-Luzarraga, K. Hodivala-Dilke, Molecular Pathways: Endothelial Cell FAK-A Target for Cancer Treatment, Clinical Cancer Research , 22 (2016) 1078-0432.

[17] G.R. Ott, M. Cheng, K.S. Learn, J. Wagner, D.E. Gingrich, J.G. Lisko, M. Curry, E.F. Mesaros, A.K. Ghose, M.R. Quail, Discovery of Clinical Candidate CEP-37440, a Selective Inhibitor of Focal Adhesion Kinase (FAK) and Anaplastic Lymphoma Kinase (ALK), J. Med. Chem., 59 (2016) 7478-7496.

[18] N.F. Brown, M. Williams, H.T. Arkenau, R.A. Fleming, J. Tolson, L. Yan, J. Zhang, L. Swartz, R. Singh, K.R. Auger, A Study of the Focal Adhesion Kinase Inhibitor GSK2256098 in Patients with Recurrent Glioblastoma with Evaluation of Tumor Penetration of [11C]GSK2256098, Neuro Oncol., 20 (2018) 1634-1642.

[19] J.B. Stokes, S.J. Adair, J.K. Slackdavis, D.M. Walters, R.W. Tilghman, E.D. Hershey, B. Lowrey, K.S. Thomas, A.H. Bouton, R.F. Hwang, Inhibition of Focal Adhesion Kinase by PF-562,271 Inhibits the Growth and Metastasis of Pancreatic Cancer Concomitant with Altering the Tumor Microenvironment, Mol. Cancer Ther., 10 (2011) 2135-2145.

[20] H.M. Lin, B.Y. Lee, L. Castillo, C. Spielman, J. Grogan, N.K. Yeung, J.G. Kench, P.D. Stricker, A.M. Haynes, M.M. Centenera, Effect of FAK inhibitor VS-6063 (defactinib) on docetaxel efficacy in prostate cancer, Prostate, 78 (2018) 308-317.

[21] Y. Su, R. Li, X. Ning, Z. Lin, X. Zhao, J. Zhou, J. Liu, Y. Jin, Y. Yin, Discovery of 2,4-diarylaminopyrimidine derivatives bearing dithiocarbamate moiety as novel FAK inhibitors with antitumor and anti-angiogenesis activities, Eur. J. Med. Chem., 177 (2019) 32-46.

[22] L. Wang, M. Ai, J. Yu, L. Jin, C. Wang, Z. Liu, X. Shu, Z. Tang, K. Liu, H. Luo, Structure-based modification of carbonyl-diphenylpyrimidines (Car-DPPYs) as a novel focal adhesion kinase (FAK) inhibitor against various stubborn cancer cells, Eur. J. Med. Chem., 172 (2019) 154-162.

[23] K.W. Temburnikar, S.C. Zimmermann, N.T. Kim, C.R. Ross, C. Gelbmann, C.E. Salomon, G.M. Wilson, J. Balzarini, K.L. Seley-Radtke, Antiproliferative activities of halogenated thieno[3,2-d]pyrimidines, Biorg. Med. Chem., 22 (2014) 2113-2122.

[24] R.J. Burton, M.L. Crowther, N.J. Fazakerley, S.M. Fillery, B.M. Hayter, J.G. Kettle, C.A. Mcmillan, P. Perkins, P. Robins, P.M. Smith, Highly regioselective Buchwald–Hartwig amination at C-2 of 2,4-dichloropyridine enabling a novel approach to 2,4-bisanilinopyridine (BAPyd) libraries, Tetrahedron Lett., 54 (2013) 6900-6904.

[25] X.M. Wang, M.H. Xin, J. Xu, B.R. Kang, Y. Li, S.M. Lu, S.Q. Zhang, Synthesis and antitumor activities evaluation of m-(4-morpholinoquinazolin-2-yl)benzamides in vitro and in vivo, Eur. J. Med. Chem., 96 (2015) 382-395.

[26] G. Ling-Jie, K. Sona, S. Michal, R. Anna Teresa, D.J. Steven, H. Piet, Discovery of dual death-associated protein related apoptosis inducing protein kinase 1 and 2 inhibitors by a scaffold hopping approach, J. Med. Chem., 57 (2014) 7624-7643.

[27] R. Wang, Y. Chen, X. Zhao, S. Yu, B. Yang, T. Wu, J. Guo, C. Hao, D. Zhao, M. Cheng, Design, synthesis and biological evaluation of novel 7*H*-pyrrolo[2,3-*d*]pyrimidine derivatives as potential FAK inhibitors and anticancer agents, Eur. J. Med. Chem., 183 (2019).

[28] M. Qu, Z. Liu, D. Zhao, C. Wang, J. Zhang, Z. Tang, K. Liu, X. Shu, H. Yuan, X. Ma, Design, synthesis and biological evaluation of sulfonamide-substituted diphenylpyrimidine derivatives (Sul-DPPYs) as potent focal adhesion kinase (FAK) inhibitors with antitumor activity, Biorg. Med. Chem., 25 (2017) 3989-3996.

[29] B. Zhou, G.Z. Wang, Z.S. Wen, Y.C. Zhou, Y.C. Huang, Y. Chen, G.B. Zhou, Somatic Mutations and Splicing Variants of Focal Adhesion Kinase in Non-Small Cell Lung Cancer, J. Natl. Cancer Inst., 110 (2018) 195-204.

[30] V. Gabarra-Niecko, M.D. Schaller, J.M. Dunty, FAK regulates biological processes important for the pathogenesis of cancer, Cancer Metastasis Rev., 22 (2003) 359-374.

- A series of thieno[3,2-*d*]pyrimidine derivatives were designed and synthesized.
- Most compounds suppressed the enzymatic activities of FAK with IC_{50} values of 10^{-7}–10^{-8} M.
- **26f** displayed stronger potency than TAE-226 in U-87MG, A-549 and MDA-MB-231 cells.
- **26f** promoted apoptosis and suppressed the migration of MDA-MB-231 cells.
- **26f** arrested MDA-MB-231 cells in the G0/G1 phase.

Declaration of interests

☒ The authors declare that they have no known competing financial interests or personal relationships that could have appeared to influence the work reported in this paper.

☐The authors declare the following financial interests/personal relationships which may be considered as potential competing interests: